Characterizing the Role of Deubiquitination in Ribosome Biogenesis

Lauren Alexandria Richardson

A dissertation submitted in partial fulfillment of the requirements for the degree of

Doctor of Philosophy

University of Washington

2012

Program Authorized to Offer Degree:
Pharmacology

University of Washington

Abstract

Characterizing the Role of Deubiquitination in Ribosome Biogenesis

Lauren Alexandria Richardson

Chair of Supervisory Committee:

Assistant Professor Richard Gardner

Department of Pharmacology

Eukaryotic ribosome biogenesis requires hundreds of trans-acting factors and dozens of RNAs. Although most factors required for ribosome biogenesis have been identified, little is known about how they are regulated. Here, we reveal that the yeast deubiquitinating enzyme Ubp10 is predominantly localized to the nucleolus and *ubp10*Δ cells have a significant reduction in pre-rRNAs, mature rRNAs, and translating ribosomes. Through proteomic analyses, we found that Ubp10 interacts with proteins that function in rRNA production and ribosome biogenesis. In particular, we discovered that the largest subunit of RNA polymerase I (RNAPI) is stabilized via Ubp10-mediated deubiquitination, and this is required to achieve optimal levels of ribosomes and cell growth. USP36, the human homolog of Ubp10, similarly regulates RNAPI in human cells and complements the *ubp10*Δ allele for RNAPI stability and cell growth in yeast. Thus, stabilization of RNAPI through deubiquitination is conserved in eukaryotes. Additionally, we proposed other potential roles for Ubp10-mediated regulation in essential nucleolar functions. Our work now places Ubp10/USP36 as a key regulator of rRNA production.

TABLE OF CONTENTS

LIST OF FIGURES

Figure Number

LIST OF TABLES

Table Number

ACKNOWLEDGEMENTS

I would like to thank my mentor Dr. Richard Gardner for his continuous support and guidance throughout my graduate career. I would also like to acknowledge Dr. Tom Milac for his help with the analysis of the proteomics data and for being a great personal advocate. I thank Dr. Richard Gardner, Dr. Edith Wang, Dr. Matt Kaberlein, Dr. Ted Young, and Dr. Ning Zheng for their excellent advice and support as my thesis supervisory committee. A special thanks goes out to all the past and present members of the Gardner Lab, particularly Melissa Locke, Ben Reed, Pamela Gallagher, Michelle Oeser, Eric Frederickson, and Joel Rosenbaum. I would also like to thank my family for their constant support and encouragement, as well as unerring faith in me and my abilities. Finally, I would like to thank my partner Jason, whose love and support has been essential and appreciated.

DEDICATION

I dedicate my dissertation to my family. There are no words to describe how much love and support they have given me over the years. Without them, none of this would have been possible.

CHAPTER I: BACKGROUND AND SIGNIFICANCE

The required regulation of ribosome biogenesis

The process of ribosome biogenesis is one of the most energetically costly in the eukaryotic cell. It is also of critical importance, as ribosomes are the machines that create all proteins. In the budding yeast, *Saccharomyces cerevisiae*, up to 80% of the RNA generated is ribosomal RNA (rRNA), and 50% of RNA polymerase II – transcription events are of ribosomal protein genes, allowing the dividing cell to synthesize approximately 2000 new ribosomes per minute (Warner, 1999). In addition to being energetically costly, ribosome biogenesis is also extremely complex, requiring over 150 trans-acting proteins and dozens of RNA molecules (Henras et al., 2008).

Ribosome biogenesis begins in the nucleolus, where, in yeast, the ribosomal DNA (rDNA) is arrayed in tandem repeats on the right arm of chromosome XII. The rDNA is transcribed by RNA Polymerase I (RNAPI), which produces a large precursor rRNA, termed the 35S rRNA. The mature rRNA species, the 18S, 5.8S, and 25S rRNAs, are released after a complex series of cleavages that involve both exo- and endo-nucleolytic digestions. The 18S rRNA forms the core of the 40S, or small subunit, while the 5.8S and 25S rRNAs, along with the 5S rRNA, which is transcribed by RNA Polymerase III, form the 60S, or large subunit (Venema and Tollervey, 1999). As RNAPI transcribes the rRNA, the nascent rRNA moiety associates with numerous complexes that eventually form the 90S pre-ribosome. The 90S pre-ribosome is a large macromolecular

complex composed of the approximately 80 ribosomal proteins and over 150 associated proteins and small nucleolar RNAs (snoRNAs) (Bernstein et al., 2004). This complex aids in the correct folding, modification and cleavage of the rRNA. The 90S pre-ribosome splits into the pre-40S and the pre-60S pre-ribosomal particles, which are then exported from the nucleoplasm. Final maturation and assembly occurs in the cytoplasm (Vanrobays et al., 2001).

Unsurprisingly, given its complexity and importance, ribosome biogenesis is thought to be a tightly regulated process. However, despite the genomic and proteomic screens that have identified the vast majority of proteins that are involved in ribosome biogenesis (Henras et al., 2008), the function and regulation of most of these factors is completely unknown.

The extant protein population is regulated by ubiquitination

One of the most prevalent means for a cell to exert control on its protein population is by ubiquitination. The covalent attachment of the small peptide ubiquitin to a substrate can affect numerous aspects of that protein's physiology, including its stability, localization, activity and/or interactions with other proteins. Ubiquitin can be attached to a protein either singly or in multi-ubiquitin chains. The linkages between ubiquitin moieties within a chain can also affect the final physiological outcome of the ubiquitination (Ciechanover, 2006).

Ubiquitin is added to substrates by an enzymatic cascade, beginning with the activation of the ubiquitin moiety by the ubiquitin activating enzyme (UBA or E1). The UBA forms a thioester linkage to ubiquitin, which requires the catalysis

of a molecule of ATP, then transfers the ubiquitin through a similar linkage to the ubiquitin conjugating enzyme (UBC or E2). The UBC coordinates with the ubiquitin protein ligase (UBPL or E3) to catalyze the transfer of the ubiquitin onto a lysine residue on the substrate. In general, the substrate specificity is encoded by the UBPL. Multicellular eukaryotes have a few UBAs, dozens of UBCs and hundreds of UBPLs, which are responsible for the ubiquitination of thousands of cellular substrates (Ciechanover, 2006).

The effect of ubiquitination on a protein depends on several factors, one being the architecture of the ubiquitin chain. Ubiquitin has seven lysine residues, each able to form a chain with another ubiquitin molecule. A chain of four or more ubiquitin moieties linked through lysine 48 residues signals the substrate protein to be degraded by the proteasome (Chau et al., 1989). Lysine 63 chains are non-degradative and have been implicated in such processes as DNA repair and stress response (Spence et al., 1995). Lysine 11 chains are important for endoplasmic reticulum associated degradation (Xu et al., 2009). Mono-ubiquitination also encodes signaling information. Histones are mono-ubiquitinated, and this is an important precursor to the activation of chromatin (Wright et al.). Additionally, many transmembrane receptors are mono-ubiquitinated, which alters their subcellular localization and often targets the receptors to destruction by the lysosome (Barriere et al., 2007). Different ubiquitin chains and mono-ubiquitin are able to exert their particular means of regulation due to the specificity of ubiquitin receptors. The binding domains of these receptors conform to fit the distinct three-dimensional conformations that

each chain creates (Ciechanover, 2006). This allows for the vast diversity of ubiquitin signaling.

Deubiquitinases are a critical modulator of ubiquitin signaling

Ubiquitination is a dynamic means of regulation, and the modification is reversed by the action of the deubiquitinases (DUBs), of which there are approximately 20 in budding yeast and approximately 100 in humans (Reyes-Turcu et al., 2009). DUBs are isopeptidases, and in humans are categorized into five gene families: ubiquitin C-terminal hydrolases, ubiquitin-specific peptidases, ovarian tumor domain proteins, Josephin or Machado-Joseph disease proteins and the JAMM domain proteins, and the monocyte chemotactic protein-induced protein. All classes are cysteine peptidases, except for the JAMM proteins, which are zinc metalloisopeptidasaes.

DUBs have numerous functions in regard to ubiquitin signaling. First, as ubiquitin is transcribed and translated as fusion between either ribosomal proteins or itself, a DUB must cleave these fusion proteins to liberate free ubiquitin moieties. DUBs must also remove ubiquitin from proteasomal substrates before degradation, and keep the proteasome free of ubiquitin chains. The proofreading of protein ubiquitination and ubiquitin chains is another key function of DUBs, as inappropriate ubiquitination must be reversed. Lastly, DUBs are also involved in maintaining the cellular pool of free ubiquitin (Wilkinson, 1997).

The extent of DUB-mediated regulation of protein function has been recently exemplified by several studies aiming to identify all the proteins that interact with DUBs in humans (Sowa et al., 2009) and in *Schizosaccharomyces pombe* (Kouranti et al., 2010). Both studies revealed hundreds of novel interacting proteins, and implicated regulation by DUBs in nearly every aspect of cellular biology. However, both of these studies suffer from the same set of limitations. First, by targeting the identification of interacting proteins, they cannot distinguish between the substrates of the DUB and the proteins that simply physically interact with it. This is critical, as the only way to truly understand the function of a DUB is to known what proteins it deubiquitinates *in vivo*. Along with this, both studies used non-denaturing coimmunoprecipitations to capture interacting proteins. This methodology may be too stringent to capture substrates, as many substrate/enzyme interactions are exceedingly transient. Most DUBs have unknown or vague cellular roles. This is due to the difficulty of identifying the cohort of substrates for any given DUB. While understanding what proteins interact with a DUB is good evidence to what cellular processes a DUB might be involved in, the best means of understanding its function is to identify its substrates.

The roles of deubiquitinases in disease

Unsurprisingly, given their critical regulation of numerous cell functions, dysregulation of DUBs can lead to disease. One of the most well characterized examples of this is the role of DUBs in cancer. DUBs have been described as

both oncogenes and tumor suppressors, and their affect on carcinogenesis is dependent on their substrates. For example, the DUB USP2a may act as an oncogene by deubiquitinating and stabilizing fatty-acid synthase, an anti-apoptotic protein, aiding in tumor cell survival (Graner et al., 2004).

DUBs have also been implicated in other diseases, such as Parkinson's Disease (PD). The ubiquitin C-terminal hydrolase isozyme L1 (UCHL1) is an abundant neuronal DUB that has also been shown to have ubiquitin ligase activity. Interestingly, mutations in UCHL1 have been found to be both protective and promoting PD, with those mutations leading to increased DUB activity of UCHL1 being protective against PD (Ardley et al., 2004; Das et al., 2006). Another neurodegenerative disease linked to a DUB is spinocerebellar ataxia type 3, which is a polyglutamine expansion disease. The disease protein in this case is Ataxin-3, a DUB. Normally, Ataxin-3 has a span of 12 to 40 glutamines near its C-terminus, yet in the disease state, this span is increased to 55 to 84 glutamines. Expression of this mutant DUB leads to neurodegeneration of the cerebellum, substantia nigra and pontine nuclei (Paulson et al., 1997). However, it has been proposed that expression of this disease gene alone is not enough to incite the specific neurodegeneration that is seen in the disease, and that other cell-specific factors must be involved (Colomer Gould, 2005).

Many viruses have evolved mechanisms to disrupt or hijack the ubiquitin signaling pathway to contribute to their virulence, and recently researchers identified a virus which encodes its own DUB. The Turnip Yellow Mosaic Virus protects its own replicative polymerase from degradation by the host ubiquitin

proteasome system by providing a viral protein which deubiquitinases the polymerase, leading to its increased stability, and increased transcription of the viral RNA (Chenon et al.).

Clearly, the role of DUBs in disease is specific to each DUB and its substrates. This highlights the need for techniques to identify a particular DUBs cohort of substrates, as this would be able to shed light on the molecular basis of ubiquitin-associated diseases.

The known nuclear role of the yeast DUB Ubp10

Ubp10 was originally identified as a *Disrupter of Telomeric Silencing* gene (formerly known as Dot4). Deletion or overexpression of Ubp10 leads to altered levels of silencing at the telomeres and other silent chromatin regions (Singer et al., 1998). In yeast, silencing at the telomeres is dependent on the Sir (Silent Information Regulator) proteins. These proteins bind to histones lacking post-translational modifications (Aparicio et al., 1991). Histones can be modified by a variety of moieties, including methyl-, acetyl-, and phospho-groups. Histones can also be ubiquitinated, primarily on the H2B subunit, by Rad6/Bre1 (Kao et al., 2004; Robzyk et al., 2000). The ubiquitination of H2B is an essential precursor for the methylation of H3 by the methyltransferases Dot1 and Set1 (Ng et al., 2002b; Sun and Allis, 2002), which methylate H3 at lysines 79 and 4, respectively. Methylation of H3 at both of these regions is associated with active chromatin (Ng et al., 2003; Ng et al., 2002a; Noma and Grewal, 2002; van Leeuwen et al., 2002).

Ubp10's mechanism of action in the context of chromatin is to remove ubiquitin from histone H2B (Emre et al., 2005; Gardner et al., 2005b). Ubp8 also deubiquitinates H2B, and is a member of the transcription complex SAGA (Henry et al., 2003). Disruption of Ubp8 has no affect on silencing, so its role is thought to be distinct from that of Ubp10. By deubiquitinating H2B at the telomeres, Ubp10 contributes to the maintenance silencing in two ways: first, it is removing a modification that itself can block Sir protein binding, and second, it prevents the methylation of H3 by Dot1 and Set1 (Emre et al., 2005; Gardner et al., 2005b). This methylation is a long-lasting histone modification, in that it is not rapidly reversed and is heritable (Ng et al., 2002a). Thus, the deubiquitination of H2B is important to repress the methylation H3, allowing for maintained silencing at the telomeres.

Ubp10 also has a proposed role in active chromatin. Gardner et al., (2005) showed that gene expression throughout both silent and active chromatin were altered in the absence of Ubp10. This effect was not due to the activation of telomeric genes, as a mutant of Ubp10, Ubp10$^{\Delta 94\text{-}250}$, which does not interact with Sir4 (Kahana and Gottschling, 1999) and thus is not localized to the telomeres, shows only changes in gene expression in silent chromatin, indicating that the Ubp10$^{\Delta 94\text{-}250}$ mutant is still able maintain its role in active chromatin. Recently, Schultze et al., (2011) found that Ubp10 deubiquitinates H2B in active chromatin, but that Ubp10 and Ubp8 deubiquitinate distinct pools of H2B. Further research is required to determine the exact role of Ubp10 in the regulation of chromatin.

Abbreviations: rRNA, ribosomal RNA; rDNA, ribosomal DNA; RNAPI, RNA polymerase I; snoRNA, small nucleolar RNA; UBA, ubiquitin activating enzyme; UBC, ubiquitin conjugating enzyme; UBPL, ubiquitin protein ligase; DUB, deubiquitinase; JAMM, JAB1/MPN/Mov34 metalloenzyme; PD, Parkinson's Disease; UCHL1, ubiquitin C-terminal hydrolase 1; SAGA, Spt-Ada-Gcn5-acetyltransferase.

CHAPTER II: ESTABLISHING A NUCLEOLAR ROLE FOR UBP10

INTRODUCTION

Ubp10 is an important enzyme in the regulation of silencing at the telomeres. However, several studies aimed at identifying all the protein-protein interactions in the cell either by tandem-affinity coimmunoprecipitation (coIP) (Krogan et al., 2006) or by protein complementation (Tarassov et al., 2008), showed Ubp10 to be interacting with numerous proteins unrelated to chromatin silencing. Also, due to the substrate promiscuity Ubp10 exhibits *in vitro* (Schaefer and Morgan); (Amerik and Hochstrasser, 2004), it is likely that Ubp10 deubiquitinates other cellular proteins (Marfany and Denuc, 2008). We hypothesized that Ubp10 may have a function independent of telomeric silencing and the Silent Information Regulator (Sir) proteins.

To determine novel roles of Ubp10 we further defined the *ubp10*Δ phenotype and we completed two proteomic screens to identify interacting proteins and substrates of Ubp10. These techniques revealed that Ubp10 is involved in nucleolar function and is required for optimal ribosome biogenesis.

MATERIALS AND METHODS

Yeast strains and plasmids. All yeast strains and plasmids are described in Appendix I. Standard yeast genetic methods were used in these studies (Guthrie and Fink, 1991).

Cell-cycle analysis. Yeast cell-cycle analyses were conducted similar to those previously described (Haase and Reed, 2002). Cell cultures were grown to ~0.8x10^7 cells/ml, harvested by centrifugation, fixed in 70% ethanol, washed in 50 mM sodium citrate containing 0.25 mg/ml RNAse A, incubated at 95˚C for 15 minutes and then 37˚C for 2 hours. Fixed cells were resuspended in 50 mM sodium citrate, stained with 2 µM SYTOX green, and sonicated for 1 second before analysis by flow cytometry. G1 and G2 phase analyses was done with WinCycle Software.

Fluorescence microscopy. Cells were grown in 5 ml cultures to a density of ~1.8x10^7 cells/ml. Harvested cells were fixed with 4% paraformaldehyde in 0.1 M sorbitol for 15 minutes, washed once with wash buffer (1.2 M sorbitol, 0.4 M KPO_4), stained with DAPI for 5 minutes in wash buffer plus 2% Triton X-100 and washed two times in wash buffer. Cells were imaged on a Nikon Eclipse 90i with a 100X objective (DIC N2 N.A. 1.4), filters for green (ET470/40x, T495LP, ET525/50m) or red (ET560/40x, T585LP, ET630/75m) fluorescence, and a Photometrics Cool Snap HQ2 cooled CCD camera with NIS-Elements acquisition software. All images were processed using Photoshop CS (Adobe Systems Inc.).

Polysome analysis. Polysome analyses were performed similar to previously described (Steffen et al., 2008). Cultures grown to ~1x10^7 cells/ml were rapidly chilled with crushed, frozen YPD containing 100 µg/ml cycloheximide. All

reagents were kept on ice and all steps performed at 4˚C. Harvested cells were washed once with 10 ml lysis buffer (25 mM Tris-HCl, pH 7.5, 40 mM KCl, 7.5 mM $MgCl_2$, 1 mM DTT, 0.5 mg/ml heparin, 100 µg/ml cycloheximide). Cells were resuspended in 1 ml lysis buffer and vortexed with glass beads to lyse. Detergents (1% final concentration of Triton X-100 and sodium deoxycholate) were added with vortexing and samples were incubated on ice for 5 minutes. Supernatants were clarified by centrifugation. Twenty A260 units of lysate in 1 ml total volume was loaded onto 11 ml linear 7%–47% sucrose gradients in 50 mM Tris-HCl, pH 7.5, 0.8 M KCl, 15 mM MgCl2, 0.5 mg/ml heparin, and 100 µg/ml cycloheximide. Gradients were centrifuged at 39,000 rpm at 4˚C in a SW40 Ti swinging bucket rotor (Beckman) for 2 hours. Gradients were collected from the top and profiles read at 254 nm.

Northern blot analysis. Northern blot analysis was performed similarly to previously described (Pestov et al., 2008). Cultures were grown at 17°C in glucose medium for 72 hours for genetic depletion of the tagged protein. Cultures were grown, kept in log phase by frequent dilution with fresh media, to a final density of 0.53 – 0.87 $x10^7$ cells/ml and harvested by centrifugation. Total RNA was extracted by the acid phenol method (Collart and Oliviero, 1994). RNA was resuspended in formamide loading dye and 3 µg was loaded per lane. pre-RNAs were separated on an agarose-formaldehyde gel and transferred to a Hybond XL membrane. Methylene blue staining was used to detect the mature 18S and 25S rRNAs. Oligonucleotide probes used to detect pre-rRNAs are: **b** 5′GCT CTT

TGC TCT TGC C, **c** 5′CCT CTG GGC CCC GAT TGC TCG AA, and **e** 5′GGC CAG CAA TTT CAA GT.

Formaldehyde crosslinking coimmunoprecipitation. Crosslinking experiments were conducted similar to those previously described (Rosenbaum et al., 2011). Cultures were grown to ~1.8x10^7 cells/ml. Formaldehyde was added to a final concentration of 1% (v/v), and cultures incubated for 5 minutes at 30˚C. Crosslinking was quenched with glycine added to a final concentration of 125 mM. Harvested cells were lysed in SUME buffer (8 M Urea, 1% SDS, 10 mM MOPS pH 6.8, 10 mM EDTA) and lysates were diluted 1:5 in IP buffer (15 mM Na_2HPO_4, 150 mM NaCl, 2% Triton X-100, 0.1% SDS, 0.5% deoxycholate, 10 mM EDTA). Lysates were incubated with 1:1000 mouse anti-HA antibody (Novagen) preconjugated to 1.25 mg/ml Protein A Dynabeads (Invitrogen) for 16 hours at 4˚C. Beads were washed three times with IP buffer and proteins were eluted by incubation at 65˚C for 10 minutes in 50 µl SUMEB (SUME + 0.01% bromophenol blue).

Ubiquitin proteome purification. Cultures were grown to ~1.8x10^7 cells/ml. Harvested cells were lysed in 5 ml denaturing lysis buffer (8 M Urea, 50 mM Tris pH 9.0, 0.05% SDS, 10 mM PMSF, 10 mM NEM). Lysates were diluted 1:5 in lysis buffer and incubated for 16 hours at 4˚C with 5 ml TALON resin (Clontech). Resin was washed twice with 10 ml lysis buffer and proteins eluted with 5 ml lysis buffer plus 50 mM EDTA. Eluate was concentrated to 50 µl.

Trypsin digestion of gel slices for MS/MS. Individual gel slices were placed in 1.5 ml tubes (Eppendorf) and consecutively washed on an orbital shaker at room temperature with water (15 minutes), 50% acetonitrile (15 minutes), and 100% acetonitrile (5 minutes) by adding enough of the wash solution to cover the gel slice and removing the wash solution after each incubation period. A solution of 100 mM ammonium bicarbonate was added, and after 5 minutes an equal volume of 100% acetonitrile was added and washing took place for 15 minutes. After removing the final wash solution, the gel slices were dried thoroughly by vacuum centrifugation. The gel slices were then cooled on ice and an ice-cold solution of 12.5 ng/µl sequencing grade trypsin (Promega) in 50 mM ammonium bicarbonate was added to cover the gel slices and incubated on ice for one hour. The remaining trypsin solution was discarded and replaced with 50 mM ammonium bicarbonate and incubated overnight at 37˚C. Following digestion, the supernatants were collected and the gel slices were washed with 0.1% trifluoroacetic acid, and after 1 hour an equal volume of acetonitrile was added followed by washing for an additional 1 hour. The original digestion supernatant and the wash for a single sample were combined into a single tube and dried by vacuum centrifugation. The digestion products were desalted using Ziptips (Millipore) per the manufacturer's instructions and dried by vacuum centrifugation.

MS/MS analyses. Dried peptide mixtures were resuspended in 7 µL of 0.1% formic acid and 5 µL was analyzed by LC/ESI MS/MS with a nano2D LC

(Eksigent) coupled to either an LTQ-FT or LTQ-OrbiTrap mass spectrometer (ThermoElectron) using a “vented” instrument configuration as described (Licklider et al., 2002), and a chromatographic solvent system consisting of 0.1% formic acid in water (A) and 0.1% formic in 100% acetonitrile (B). In-line de-salting was accomplished using an IntegraFrit trap column (100 µm × 25 mm; New Objective) packed with reverse phase Magic C18AQ (5 µm, 200 Å resin; Michrom Bioresources) followed by peptide separations on a PicoFrit column (75 µm × 200 mm; New Objective) packed with reverse phase Magic C18AQ (5 µm, 100 Å resin; Michrom Bioresources) directly mounted on the electrospray ion source. A 90-minute non-linear gradient was used starting at 5% B. The percentage of acetonitrile was increased to 7% B over 2 minutes, then 35% B over 90 minutes. The acetonitrile percentage was increased to 50% B over 1 minute then held at 50% B for 9 minutes followed by ramping to 95% B over 1 minute, held at 95% B for 5 minutes, then decreased to 5% B over 1 minute. A flow rate of 400 nl/minute was used for chromatographic separations and the mass spectrometer capillary temperature was set to 200^{o}C. The mass spectrometers were operated in the data-dependent mode, switching automatically between MS survey scans in the FT or OrbiTrap with MS/MS spectra acquisition in the linear ion trap. The 5 most intense ions from the Fourier-transform (FT) full scan were selected in the linear ion trap for fragmentation by collision-induced dissociation with normalized collision energy of 35%. Selected ions were dynamically excluded for 45 seconds.

Mass spectrometry and data analysis. Samples analyzed by MS/MS were run 1 cm into an 8-16% SDS-PAGE gel and gel slices excised. Proteins in the gel slices were digested with trypsin (see Supplemental Experimental Procedures). The digestion products were desalted and dried by vacuum centrifugation. Dried peptide mixtures were resuspended in 7 µL of 0.1% formic acid and 5 µL was analyzed by LC/ESI MS/MS using either an LTQ-FT or LTQ-OrbiTrap mass spectrometer (ThermoElectron). Complete MS/MS methods are in the Supplemental Experimental Procedures. The protein database search algorithm X!Tandem (Craig and Beavis, 2004) was used to identify peptides from the Saccharomyces Genome Database (http://www.yeastgenome.org). Peptide false discovery rates were measured using Peptide Prophet (Keller et al., 2002), and results were stored and analyzed in the Computational Proteomics Analysis System (CPAS) (Rauch et al., 2006). To apply different levels of stringency, peptides were filtered using Peptide Prophet scores of ≥0.35 (~10% error rate), ≥0.65 (~5% error rate), and ≥0.85 (~2% error rate). The data obtained after each of these filters is in Supplemental Tables S1 and S2. For Tables 1 and 2, we used the data that was filtered using a Peptide Prophet score ≥0.35. Distributions for the case and control replicates were compared using an unpaired student's t-test (with the replicate groups having equal sample size and unequal variance). Two tailed p values are reported.

RESULTS

Ubp10 acts independently from the Sir proteins

Ubp10 is necessary for optimal cell growth. Ubp10 was originally identified as a regulator of telomeric silencing (Singer et al., 1998), through its deubiquitination of histone H2B (Emre et al., 2005; Gardner et al., 2005b). However, several aspects of *ubp10*Δ cell physiology suggest that this is not its only role. *ubp10*Δ cells have a distinct slow growth phenotype that is unrelated to a loss of gene silencing (Figure 2.1 and (Kahana and Gottschling, 1999)). Deletion of *SIR2, SIR3,* or *SIR4*, all genes essential to chromatin silencing, does not result in any depression of growth rate (Figure 2.1, left panel). Previous studies identified a mutant of Ubp10 that cannot bind to Sir4, due to the deletion of residues 94-250, and is not localized to the telomeres (Gardner et al., 2005b; Kahana and Gottschling, 1999). This mutant, $Ubp10^{\Delta 94\text{-}250}$, shows disrupted telomeric silencing, but maintains a wild-type growth rate, underscoring that the loss of Ubp10's silencing function does not affect growth rate (Figure 2.1, right panel). Yet, when the catalytic activity of Ubp10 is lost due to a the mutation of its catalytic cysteine residue ($ubp10^{C371S}$), the growth defect persists (Figure 2.1, right panel), demonstrating that the catalytic activity of Ubp10 is required for optimal cell growth.

*ubp10*Δ *cells have a cell cycle abnormality.* To investigate the nature of the *ubp10*Δ growth defect, we used flow cytometry to determine the ratio of cells in an asynchronously growing culture in each phase of the cell cycle. Analysis of *ubp10*Δ cultures compared to those of *UBP10* cultures show that *ubp10*Δ cultures have an increased population of cells in G1. This defect could explain

the growth depression that is seen in *ubp10*Δ cells, as the increased population may reflect a difficulty bypassing the G1 checkpoint. Similarly, *ubp10*^{C371S} cultures also had an increased G1 population, whereas *Ubp10*$^{\Delta 94\text{-}250}$ is similar to *UBP10* levels (Figure 2.2, top row). *sir2*Δ, *sir3*Δ, and *sir4*Δ cultures also had wild-type populations (Figure 2.2, bottom row). This demonstrates that the catalytic activity of Ubp10 is required for optimal passage through G1.

Ubp10 is localized to the nucleolus. Telomeric proteins, as exemplified by Sir4, have a distinct punctate localization at the edge of the nucleus corresponding to the position of the telomeres (Figure 2.3, top panel, (Palladino et al., 1993)). Since a direct interaction with Sir4 recruits Ubp10 to the telomeres (Gardner et al., 2005b), we would suppose that Ubp10 and Sir4 would have similar localization. However, Ubp10 is seen diffusely in the cytoplasm and throughout the nucleus (Figure 2.3, bottom panel). Most striking, when colocalized with Nop58, a nucleolar protein, we see Ubp10 highly enriched in the nucleolus. The predominant nucleolar localization of Ubp10 indicates that Ubp10 likely participates in some aspect of nucleolar biology.

Ubp10 is required for optimal ribosome biogenesis

*ubp10*Δ *cells have reduced ribosomal content.* The primary function of the nucleolus is the inception of ribosome biogenesis. Here, the rDNA is transcribed and the pre-40S and pre-60S subunits are formed. Ribosome biogenesis is a critical process for the growth capacity of the cell, as a constant supply of new

ribosomes is required to produce the large amounts of proteins needed to drive DNA replication and cell division. As we know Ubp10 is localized to the nucleolus, and lack of *UBP10* leads to slow growth, we wanted to investigate if Ubp10 affects ribosome biogenesis. To do this, we used polysome analysis from cell lysates of *UBP10* and *ubp10*Δ cells to separate and visualize the free 40S and 60S subunits and the translating polysomes. By measuring the area under the curves, we found there was an approximately 30-40% reduction in the 40S and 60S subunits as well as translating ribosomes in *ubp10*Δ cells (Figure 2.4). Importantly, the ratio of the 40S to 60S subunits was maintained in *ubp10*Δ cells, suggesting an overall defect in ribosome production.

*rRNA production and processing is altered in ubp10*Δ. One of the critical processes within ribosome biogenesis is the cleavage of the large pre-rRNA molecule, the 35S, into the mature rRNA species, the 18S, 5.8S and 25S (Figure 2.5). To determine if Ubp10 plays a role rRNA processing we preformed a Northern analysis. The majority of ribosome biogenesis proteins are essential, so pre-rRNA processing analyses typically employ genetic depletion experiments. Here, the gene of interest is placed under the control of the galactose-inducible promoter *GAL1* (Dragon et al., 2002), allowing for repression of the gene upon transfer of cells to glucose growth medium. To follow in line with these experiments, we created a *GAL1::3HA-UBP10* strain. We compared the affect of genetic depletion of Ubp10 on processing with that of Utp16 and Utp25, two proteins involved in 18S processing. Genetic depletion of Ubp10

resulted in a decreased abundance of several rRNA precursor species, most notably the 35S pre-rRNA (Figure 2.6, left and middle panel). Consistent with the reduction of 40S and 60S subunits in the *ubp10*Δ polysome profiles, we also observed an approximately 40% decrease in the levels of the mature 18S and 25S rRNAs after genetic depletion of Ubp10 (Figure 2.6, right panel). By contrast, genetic depletion of Utp16 and Utp25 led to an accumulation of the 35S transcript, but depletion of the mature 18S rRNA. Overall, loss of Ubp10 resulted in a defect in 35S pre-rRNA levels, that in turn likely affects production of the large and small subunit rRNAs and reduces the total ribosome levels in the cell.

Proteomic analyses reveal a nucleolar function of Ubp10

Proteins that interact with Ubp10 are enriched in ribosome biogenesis functions. To determine the specific functional roles for Ubp10 in the nucleolus, we used a coIP tandem mass spectrometry (MS/MS) approach to survey Ubp10-interacting proteins including substrates and partners. To assure the capture of even transient interactors, such as substrates, we employed a formaldehyde crosslinking step (Sutherland et al., 2008). This also allowed us to lyse the cells under strong denaturing conditions, thus decreasing nonspecific interactions that may arise after cell lysis. To facilitate the coIP, we used a C-terminal 3HSV-tagged version of Ubp10 expressed from its native promoter. The addition of this tag did not affect Ubp10's function in silencing, histone H2B deubiquitination, or cell growth. For a negative control, we used untagged Ubp10. All coIPs were preformed in triplicate with independently grown cultures. A protein was

categorized as interacting with Ubp10 if the summed spectral (peptide) counts of the protein identified by MS/MS in the tagged replicates by ≥3-fold. Using these criteria, we identified 83 Ubp10-interacting proteins (Table 2.1, Appendix II encompasses the entire data set).

We analyzed the set of Ubp10 interactors using the cluster interpreter FunSpec (http://funspec.med.utoronto.ca/), which can reveal enrichment for cellular functions, localizations, known protein complexes, and other useful parameters (Robinson et al., 2002). Of the 83 candidates, 37 have full or partial nucleolar localization (Figure 2.7). The interactors are also highly enriched for proteins involved in ribosome biogenesis and, more specifically, in 35S pre-rRNA processing as part of the 90S pre-ribosome (Figure 2.7).

To aid in visualizing the MS/MS interaction data, we created a network of the nucleolar proteins that interact with Ubp10 (Figure 2.8). The thick lines in the network that connect Ubp10 to each protein indicate the primary interactions identified by crosslinking coIP MS/MS. The thin lines represent interactions indicated by previous studies (Dragon et al., 2002; Gallagher et al., 2004; Grandi et al., 2002; Krogan et al., 2004a; Krogan et al., 2004b; Kuhn et al., 2007; Li and Ye, 2006; Liang et al., 2009; Lim et al., 2011; Rashid et al., 2006; Reichow et al., 2007; Tarassov et al., 2008; Wittmeyer et al., 1999). From this arrangement, Ubp10 clearly interacts with numerous subcomplexes involved in 35S pre-rRNA transcription and processing. In particular, Ubp10 interacts with Rpa190, the essential largest subunit of RNA polymerase I (Memet et al., 1988), which is responsible for transcribing the 35S pre-rRNA (Russell and Zomerdijk, 2006).

Ubp10 also has several interactions with proteins of the UTP-A (also known as t-Utp), UTP-B, and UTP-C complexes, which are required for the cleavage events that liberate the 18S rRNA from the 35S pre-rRNA (Phipps et al., 2011). Ubp10 interacts with components of the Box C/D and Box H/ACA small nucleolar ribonucleoprotein particles (snoRNPs), which are involved in rRNA cleavage and modification (Reichow et al., 2007). Ubp10 also interacts with several other proteins required for small or large ribosome subunit biogenesis, including a number of key RNA helicases (Dbp2, Dbp4, Dhr2, Has1, and Prp43). Lastly, we identified histone H2B (Htb2), indicating that the method allowed for the capture of Ubp10's only known substrate.

Identifying novel substrates of Ubp10. To uncover Ubp10's nucleolar role we sought to identify novel substrates of Ubp10. The crosslinking coIP MS/MS analysis identified new proteins that interact with Ubp10, but the method did not allow us to distinguish between Ubp10 partners and substrates. Therefore, we employed a different method to identify potential Ubp10 substrates, which was to compare the isolated ubiquitin proteome from *UBP10* cells with that from *ubp10*Δ cells using MS/MS. Because Ubp10 is a deubiquitinating enzyme that removes ubiquitin from its substrates, we reasoned that Ubp10 substrates would have increased abundance in the ubiquitin proteome from *ubp10*Δ cells compared to the ubiquitin proteome from *UBP10* cells. To conduct the analysis, we used a yeast strain in which all endogenous ubiquitin genes have been deleted (Finley et al., 1994), with the sole source of ubiquitin coming from an 8-histidine tagged

ubiquitin gene expressed from the *CUP1* promoter on a high copy plasmid. We isolated the respective ubiquitin proteomes from *UBP10* and *ubp10*Δ cells by metal affinity chromatography, and ubiquitinated proteins were identified by MS/MS. Analysis of the ubiquitin proteomes was performed in triplicate using independently grown cultures of *UBP10* and *ubp10*Δ cells.

We categorized a protein as a potential Ubp10 substrate if the summed spectral (peptide) counts of the protein identified by MS/MS in the *ubp10*Δ replicates was a minimum of 4 and exceeded its summed spectral counts in the *UBP10* replicates by ≥1.5-fold. The 1.5-fold criterion in this analysis differed from the 3-fold criterion used in the crosslinking analysis because we knew that loss of Ubp10 can have subtle effects on substrate ubiquitination based on our histone H2B studies (Gardner et al., 2005b), and we wanted to increase the opportunity to identify substrates. Using the stated criteria, we identified 142 proteins that have statistically increased spectral counts in the *ubp10*Δ replicates (p value ≤ 0.1, Appendix III). As a key control, the number of peptides identified from ubiquitin is similar between the *ubp10*Δ and the *UBP10* replicates (Table 2.2), indicating that purification of the ubiquitin proteomes from *ubp10*Δ and *UBP10* cells was equivalent. Importantly, we identified Ubp10's known substrate histone H2B (Htb2) by this method (Table 2.2), verifying the method's utility for substrate discovery.

In this data set, we identified 10 proteins involved in ribosome biogenesis (Table 2.2). All of these were also identified in the crosslinking coIP analysis (Table 2.1 and Figure 2.7). When we examined the list of potential Ubp10

substrates in Table 2.2 for the protein that could best explain the phenotype of *ubp10*Δ cells, we identified Rpa190. Rpa190 is the largest, catalytic subunit of RNAPI. We could then expect that if there is dysregulation of RNAPI due to loss of Ubp10, that there would be decreased transcription of the 35S and a decreased ribosomal content, similar to what we had observed. In the next Chapter I will describe our studies of the regulation by deubiquitination of Rpa190.

DISCUSSION

While previous research has identified Ubp10 as a regulator of telomeric silencing, we have discovered a novel involvement of Ubp10 in the critical cell process of ribosome biogenesis. We showed that the growth rate defect of *ubp10*Δ cells is due to a defect in the G1 phase of the cell cycle. Interesting, this defect is common amongst proteins involved in ribosome biogenesis (Amerik et al., 2000; Delaney et al.), indicating that Ubp10 may also play a role in this process. We also show that *ubp10*Δ cells have a decreased ribosomal content, yet the ratio of free 40S to free 60S is maintained. This is important as most proteins that regulate ribosome biogenesis are specific to either the production of either subunit, hinting that Ubp10 is involved in a process that has a global biogenesis impact. This coordinates with our rRNA processing data, which shows that levels of the 35S transcript are decreased upon genetic depletion of

Ubp10 as are levels of the 18S and 25S mature rRNAs. These data suggest that Ubp10 somehow regulates the production of the 35S transcript.

The dynamic regulation of the ubiquitin signal by DUBs is clearly critical to cell functions; however, there exists no single technique to understand a DUB's function or substrates. Studies have been completed in *Schizosaccharomyces pombe* (Kouranti et al., 2010) and human cells (Sowa et al., 2009) aiming to identify all the interacting proteins for each DUB in their model organisms. These have created a compendium of interactions that can be used to guide future DUB research. Of particular note, both studies, when querying Ubp10 homologs, Ubp16 (*S. pombe*) and USP36 (*H. sapiens*), identified ribosome biogenesis proteins as interacting proteins. Particularly, they identified proteins of the UTP-B complex, of which our study identified two proteins (Pwp2 and Utp13). This suggests that the mechanism of regulation of ribosome biogenesis by Ubp10 is an evolutionarily conserved mechanism. Our studies of Ubp10 identified far more ribosome biogenesis proteins than both the Ubp16 or USP36 studies, and this is most likely due to the addition of the formaldehyde crosslinking step that we incorporated. Crosslinking stabilizes the protein-protein interactions, and aids in capturing transient interactions, such as those between substrates and enzymes. An additional benefit of our screening technique is that we combined it with our comparative ubiquitin proteome screen. The crosslinking coIP identifies proteins that physically interact with Ubp10, and these would include both substrates and binding partners. The ubiquitin proteome comparison identifies proteins with increased ubiquitination in the absence of Ubp10. These

ubiquitination events could be due to the loss of Ubp10, or due to secondary effects due to the deletion of the DUB. By combining the data from these two screens, we were able to identify substrates of Ubp10 with higher probability.

Abbreviations used: coIP, coimmunoprecipitation; FACS, fluorescence assisted cell sorting; DUB, deubiquitinase; rDNA, ribosomal DNA; rRNA, ribosomal RNA; MS/MS, tandem mass spectrometry; HSV, herpes simplex virus; snoRNP, small nucleolar ribonucleoproteins.

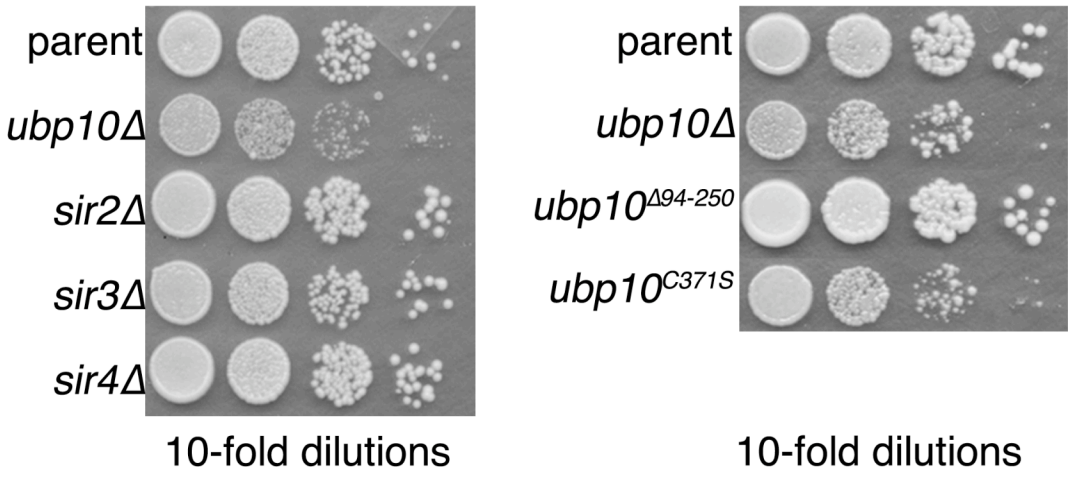

Figure 2.1: Ubp10 is required for optimal cell growth. Plate growth of a parent strain compared to *ubp10*Δ, *sir2*Δ, *sir3*Δ, *sir4*Δ, *ubp10*$^{\Delta 94\text{-}250}$, and *ubp10*^{C371S} strains. 10-fold serial dilutions of cells were spotted on rich medium and incubated at 30˚C for 3 days.

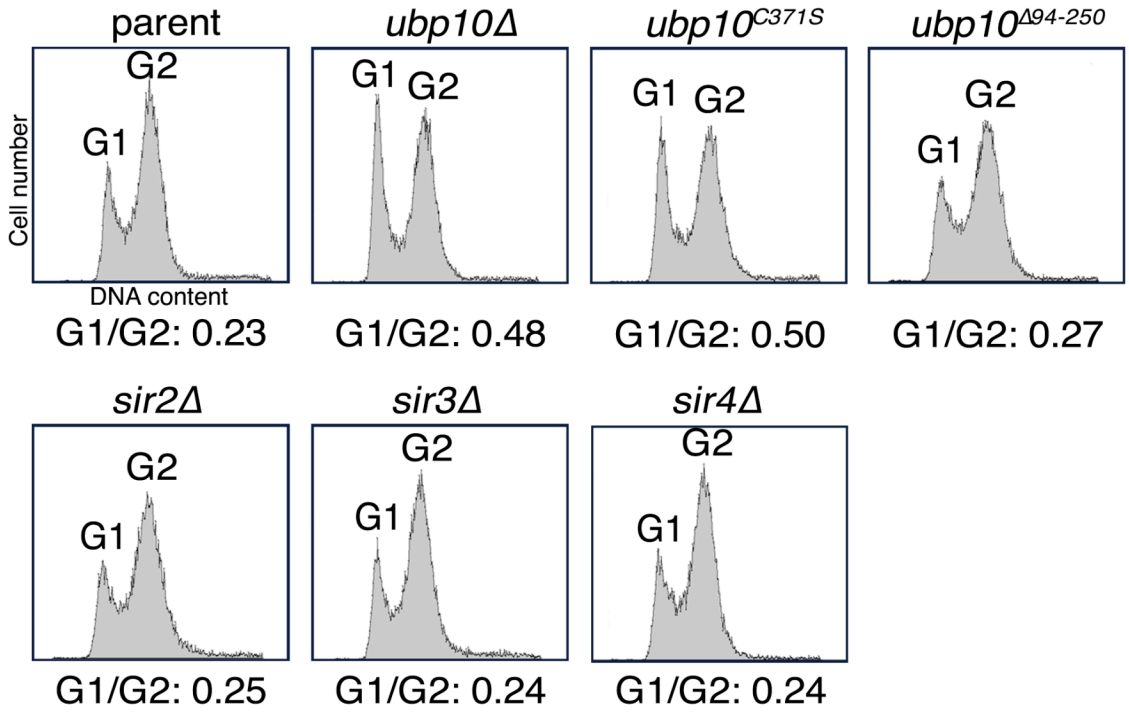

Figure 2.2: *ubp10*∆ cells have a cell cycle abnormality. Cell-cycle profiles for asynchronous cultures of a parent strain compared to *ubp10*∆, *sir2*∆, *sir3*∆, *sir4*∆, $ubp10^{\Delta 94\text{-}250}$, and $ubp10^{C371S}$ strains were examined by propidium iodide staining and flow cytometry. Proportions of cells in G1 versus G2 phases (n=3) and representative images are presented.

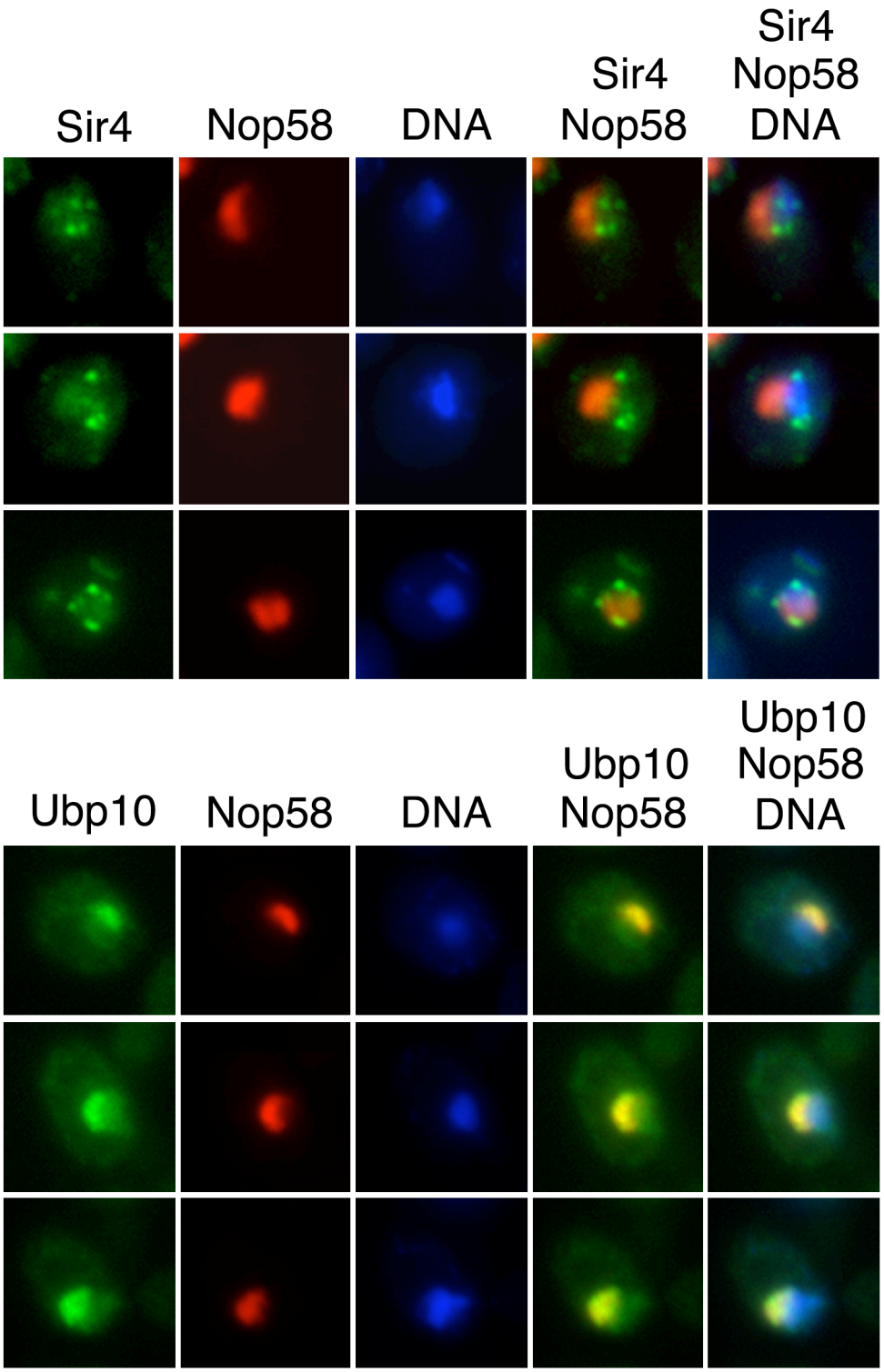

Figure 2.3: Ubp10 is predominately localized to the nucleolus. Fluorescence microscopy of exponentially growing cells co-expressing Nop58-dsRed and either Sir4-GFP or Ubp10-GFP. Nop58-dsRed marks the nucleolus and DAPI staining marks chromatin.

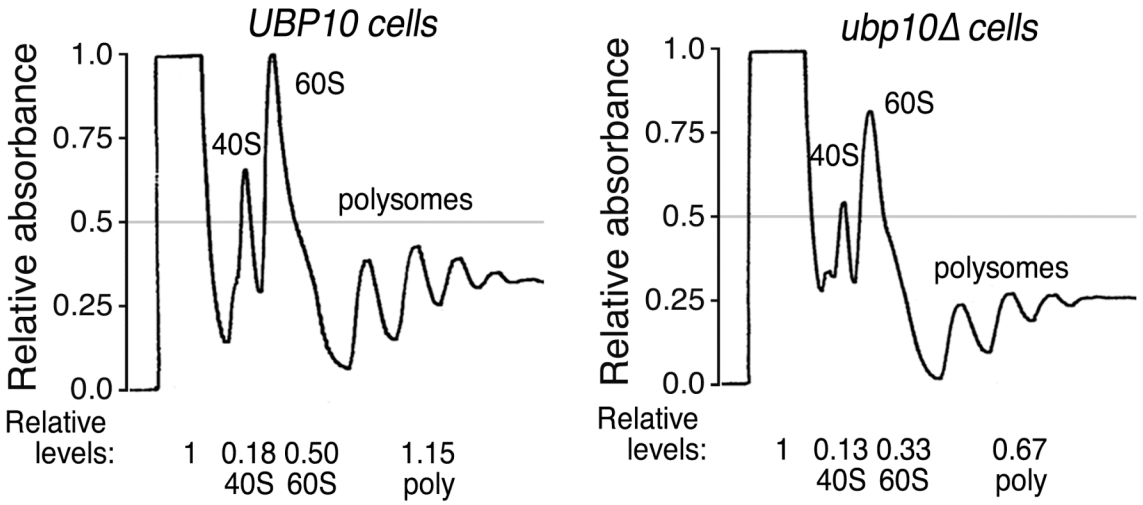

Figure 2.4: *ubp10*∆ cells have reduced ribosomal content. Polysome profiles for *UBP10* and *ubp10*∆ cells were generated from lysates of asynchronous cultures. Lysates were loaded onto 7-47% sucrose gradients and centrifuged for 1.5 hours at 39,000 rpm at 4°C. Preps were normalized to A260 units. The top of the gradient is to the left. One representative profile from three experiments shown.

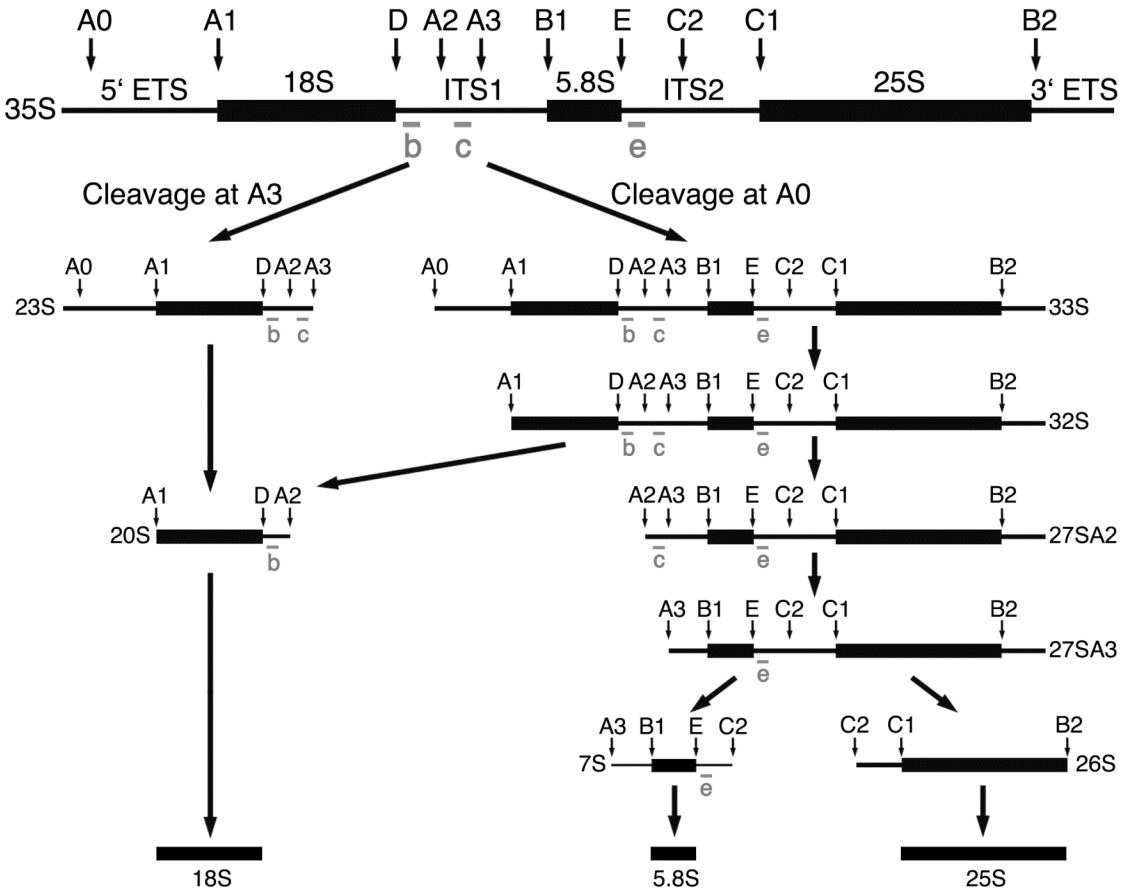

Figure 2.5: Schematic of the pre-rRNA processing pathway in yeast.

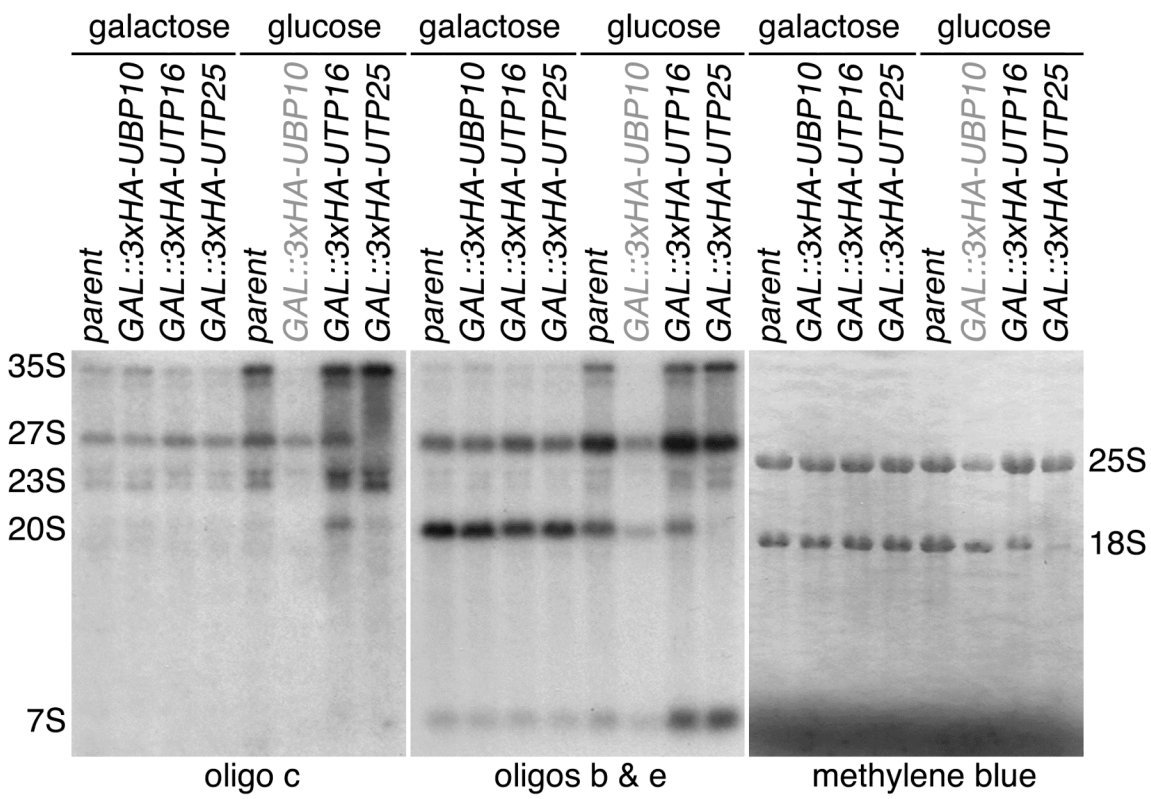

Figure 2.6: rRNA production and processing is altered in *ubp10*Δ. Genetic depletion of Ubp10 resulted in a decrease in pre-rRNA species and mature 18S and 25S rRNA. Total RNA was extracted from yeast in which the indicated protein was genetically depleted for 72 hrs at 17°C. Mature and pre-rRNA species were detected by Northern analysis using the indicated oligonucleotide probes or with methylene blue staining. The parental strain (YPH499) is shown along with *GAL1::3xHA-UTP16* and *GAL1::3xHA-UTP25* as controls.

Protein	# peptides tag	# peptides no tag	p-value	location	Protein	# peptides tag	# peptides no tag	p-value	location
Acs2	17	4	0.011	n	Nug1	4	0	0.270	n, nu
Ade3	9	1	0.105	n, c	Pol5	4	0	0.270	n, nu
Asn2	7	1	0.076	c	Prp43	16	0	0.103	nu
Bfr2	4	0	0.184	nu	Pwp1	4	0	0.057	nu
Bmh2	9	2	0.134	n, c	Pwp2	14	0	0.020	nu
Cam1	6	0	0.038	c	Pyc2	4	0	0.057	c
Cbf5	7	0	0.020	nu	Rnr2	6	1	0.082	c
Cdc48	5	1	0.267	n, c	Rnr4	4	0	0.057	n
Dbp2	21	1	0.159	nu	Rpa190	16	2	0.116	nu
Dbp4	4	0	0.057	nu	Rpl13B	8	0	0.423	c
Dbp9	4	0	0.270	nu	Rpl18A	8	0	0.157	c
Dhr2	35	0	0.022	nu	Rpl31A	9	3	0.074	c
Dph5	4	1	0.101	c	Rpl6A	9	3	0.423	c
Drs1	10	0	0.063	nu	Rpl7A	14	1	0.409	c
Fpr3	9	0	0.035	nu	Rps1A	17	4	0.060	c
Fpr4	5	0	0.199	nu	Rrp5	40	0	0.052	nu
Gcd11	10	1	0.003	c	Sec13	4	0	0.057	s
Gcn1	4	0	0.057	c	Sec4	6	0	0.074	s
Gly1	6	2	0.184	n, c	Sec53	8	1	0.246	er
Gnd1	13	0	0.006	c	Sis1	4	0	0.270	n, c
Has1	17	0	0.003	nu	Spt16	6	0	0.423	n
Hrp1	4	0	0.057	n	Sub2	9	0	0.035	n
Htb2	5	1	0.047	n	Sup45	4	1	0.101	c
Imd4	8	0	0.184	c	Swp82	5	1	0.267	n
Kre33	9	0	0.095	nu	Tkl1	28	9	0.034	n
Lys20	14	0	0.129	n	Ty1B-BL	4	0	0.423	n
Mak11	8	0	0.057	nu	Ubp10	120	0	0.001	nu, n, c
Mak21	6	0	0.184	nu	Ura2	14	4	0.191	c
Mdn1	5	0	0.300	n	Ura5	4	0	0.184	c
Mir1	6	2	0.369	m	Ura7	4	0	0.184	c
Mrd1	10	0	0.214	nu	Utp10	10	0	0.214	nu
Ncl1	4	0	0.057	n	Utp13	8	0	0.057	nu
Noc2	7	0	0.073	nu	Utp17	6	0	0.074	nu
Nog1	5	0	0.130	n	Utp22	20	0	0.017	nu
Nop1	9	3	0.225	nu	Utp4	5	0	0.199	nu
Nop12	5	0	0.038	nu	Utp7	4	0	0.057	nu
Nop4	5	0	0.130	nu	Vma13	4	1	0.101	v
Nop56	13	2	0.040	nu	Ymr099c	5	0	0.130	n
Nop58	23	3	0.031	nu	Yol077c	4	0	0.057	nu, n
Nop7	4	0	0.184	nu	Yor051c	4	0	0.057	n
Npl3	9	3	0.074	n	Yra1	6	0	0.184	n
Nsr1	14	1	0.001	nu					

c = cytoplasm, er = endoplasmic reticulum, m = mitochondria, n = nucleus, nu = nucleolus, s = secretory pathway, v = vacuole

Table 2.1: Proteins that immunoprecipitated with Ubp10 after formaldehyde crosslinking

GO Biological Process	p-value	k	f
nucleolus	<1e-14	37	476
ribosome biogenesis	<1e-14	30	192
rRNA processing	<1e-14	30	275
90S preribosome	<1e-14	18	77
35S rRNA processing	1e-09	11	73

Figure 2.7: Proteins that interact with Ubp10 are enriched in ribosome biogenesis functions. FunSpec (http://funspec.med.utoronto.ca/) analysis of the 83 interacting proteins identified by crosslinking coIP MS/MS with Ubp10-3HSV. The p-value represents the probability that the intersection of a given list with any functional category occurs by chance. "k" represents the number of genes from the input and "f" represents the total number of genes for that category in the yeast proteome.

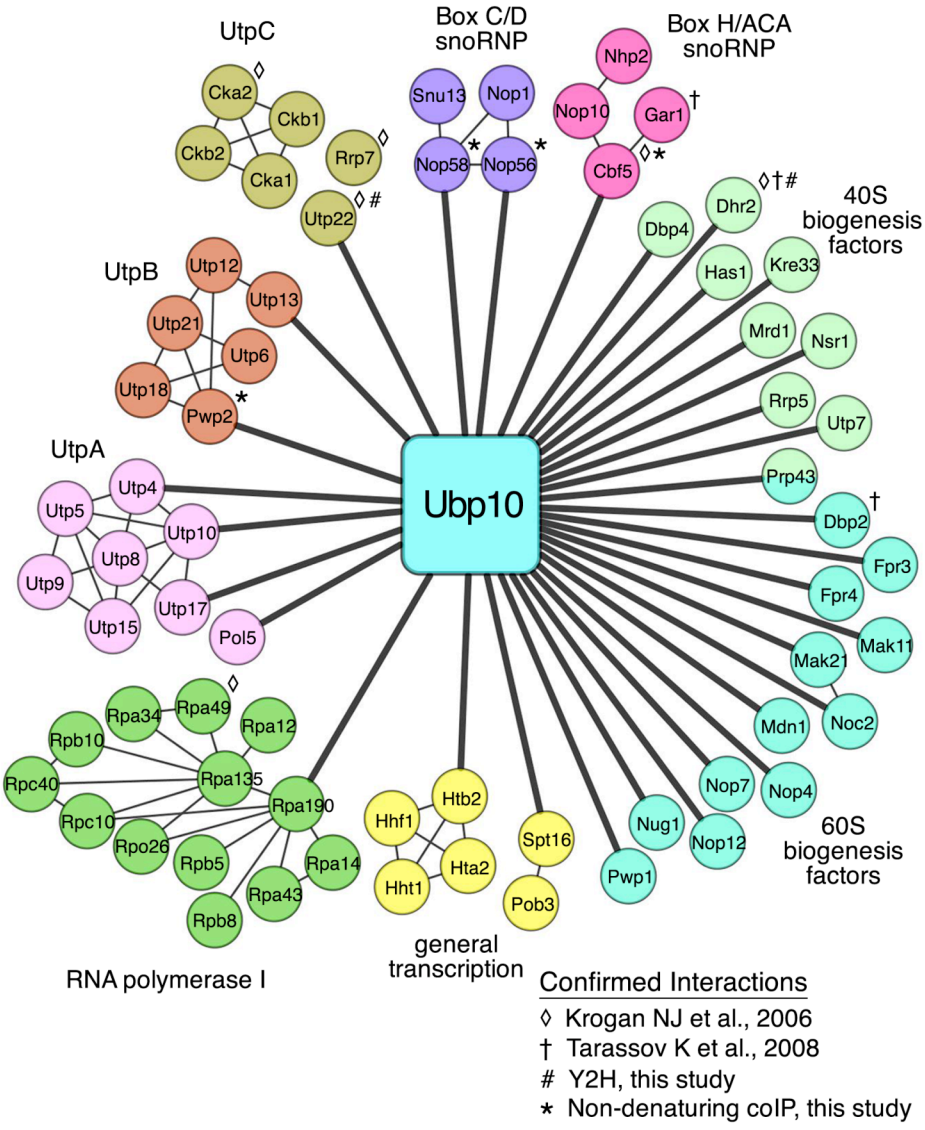

Figure 2.8: Ubp10 interacts with distinct complexes of ribosome biogenesis machinery. Network diagram of the nucleolar-localized proteins identified by crosslinking coIP MS/MS with Ubp10-3HSV. Diagram was generated using Cytoscape (http://www.cytoscape.org/) (Smoot et al., 2011). Thick lines connect interactions discovered by the crosslinking coIP MS/MS analysis. Thin lines mark interactions previously described. RNA polymerase I, BoxC/D snoRNP, and Box H/ACA snoRNP interactions were derived from solved crystal structures (Kuhn et al., 2007; Liang et al., 2009; Rashid et al., 2006; Reichow et al., 2007). UtpA, UtpB, and UtpC interactions were derived from global coIP and Y2H studies (Dragon et al., 2002; Gallagher et al., 2004; Grandi et al., 2002; Krogan et al., 2004a; Krogan et al., 2004b; Li and Ye, 2006; Lim et al., 2011; Tarassov et al., 2008; Wittmeyer et al., 1999). ◊ and † denote those interactions between Ubp10 and the target proteins that have been previously published (Krogan et al., 2006; Tarassov et al., 2008). # and * denote those interactions between Ubp10 and the target proteins that are confirmed by coIP or Y2H in Figure 4.1.

Protein	# peptides *ubp10Δ*	# peptides *UBP10*	*ubp10Δ/ UBP10* ratio	p value
Rpa190	357	137	2.61	0.002
Dbp2	6	1	6	0.025
Mak21	6	1	6	0.175
Mdn1	6	1	6	0.129
Utp10	6	1	6	0.175
Fpr3	5	1	5	0.018
Fpr4	5	0	>5	0.042
Rrp12	5	0	>5	0.042
Cbf5	4	0	>4	0.102
Has1	4	0	>4	0.102
Htb2	105	65	1.62	0.137
Ubiquitin	1734	1866	0.93	0.496

Table 2.2: Ribosome biogenesis proteins with increased abundance in the *ubp10*Δ ubiquitin proteome.

CHAPTER III: UBP10 REGULATES RNA POLYMERASE I STABILITY

INTRODUCTION

Our proteomic screens revealed a nucleolar role for Ubp10. In particular, the comparative ubiquitin proteome analysis identified Rpa190 as a potential substrate of Ubp10. The ubiquitination of Rpa190 was increased ~2.5 fold in *ubp10*Δ cells compared to *UBP10* cells. Rpa190 is the largest, catalytic subunit of RNA Polymerase I (RNAPI) (Memet et al., 1988). We wanted to determine if Ubp10 regulates Rpa190, and if this regulation could result in the decreased rRNA and ribosomes that we see in the *ubp10*Δ cells.

In addition to identifying how Ubp10 regulates Rpa190 in yeast, we also wanted to determine if this is a conserved mechanism of RNAPI regulation. The human DUB USP36 and the *Drosophila* DUB scrawny have significant homology with Ubp10 (Buszczak et al., 2009). USP36 shares 27% identity and 49% similarity with Ubp10 in the catalytic DUB domain, and scrawny shares 31% identity and 50% similarity. Interestingly, both USP36 and scrawny are predominantly nucleolar localized in human and *Drosophila* cells, respectively (Buszczak et al., 2009; Endo et al., 2009). Similar to the growth deficit we observed with *ubp10*Δ yeast cells, knockdown of USP36 levels reduced proliferation of HeLa cells (Endo et al., 2009), and deletion of scrawny reduced the proliferation of follicle and intestinal stem cells in *Drosophila* (Buszczak et al., 2009). These observations suggest that human USP36 and *Drosophila* scrawny might function analogously in modulating RNAPI stability.

MATERIALS AND METHODS

Yeast strains and plasmids. All yeast strains and plasmids are described in Appendix I. Standard yeast genetic methods were used in these studies (Guthrie and Fink, 1991).

Substrate verification. Cultures were grown to ~1x10^7 cells/ml. Harvested cells were lysed in Denaturing Lysis Buffer. Lysates were diluted 1:10 with Equilibration/Wash Buffer (300 mM NaCl, 50 mM $NaHPO_4$ pH 7.0) with 100 µl of TALON resin. Samples were incubated for 16 hours at 4˚C. Resin was washed three times with Equilibration/Wash Buffer with 7.5mM imidazole. Proteins were eluted by incubation at 65˚C for 10 minutes in 75 µl SUMEB. Proteins were separated on 8% SDS-PAGE gels, transferred to nitrocellulose, and visualized with anti-HA (Sigma) antibodies.

Cycloheximide-chase degradation assays. Cycloheximide-chase degradation assays were performed similar to previously described (Gardner et al., 2005a). Cultures were grown to a cell density of 1x10^7 cells/ml. Cycloheximide was added to a final concentration of 50 µg/ml and the cells were further incubated at 30°C for 0–3 hours. Cells were lysed at the appropriate time point in 200 µl SUMEB with 10 mM PMSF. Proteins were separated on 8% SDS-PAGE gels, transferred to nitrocellulose, and visualized with anti-HA (Sigma) antibodies.

Transfection of siUSP36 into HeLa cells. Cells were seeded into 6-well plates at 150,000 cells/well concentration 1 day before transfection. 20 nM final concentration of USP36 siRNAs (sequences are in the Supplemental Experimental Procedures) were transfected by Lipofectamine RNAiMAX (Invitrogen) according to manufacturer's protocol. The cells were subsequently incubated at 37˚C, in a 5% CO_2 incubator for 48 hours.

HeLa cell RNA extraction and real-time PCR. Total RNA was purified from cells using the Absolutely RNA miniprep kit (Stratagene) according to the manufacturer's instructions and quantified by measuring OD260. RNA samples were reverse transcribed using iScript cDNA sysnthesis kit (BioRad) and subjected to real-time PCR (RT-PCR) using Brilliant SYBR Green QPCR Master Mix (Stratagene). Description of RT-PCR reactions and primers is in the Supplemental Experimental Procedures.

HeLa cell protein extraction and immunoblotting. Cells were washed twice with 1xPBS and resuspended in RIPA buffer (50 mM Tris pH7.4, 150 mM NaCl, 0.25% sodium deoxycholate, 1% NP40, 0.1% SDS, 1 mM PMSF, 1 μg/ml aprotinin, 1 μg/ml leupeptin, 1 μg/ml pepstatin and 1 mM DTT). Cell lysates were incubated on ice for 20 minutes with vortexing every 5 minutes for 15 seconds. Cell extracts were collected after centrifugation at 14,000 rpm for 10 minutes at 4˚C to remove insoluble material. Protein concentration of whole cell extracts was determined using the Bio-Rad Protein Assay Kit according to the

manufacturer's instructions. 100 µg of total protein was separated on 10% SDS-PAGE gels, transferred to nitrocellulose, and visualized with anti-RPA194 monoclonal antibody (SC-48385, Santa Cruz Biotech), anti-USP36 polyclonal antibody (Masayuki Komada (Endo et al., 2009)), or GAPDH monoclonal antibody 6C5 (Advanced ImmunoChem Inc).

HeLa cell proliferation analysis. Cells were plated into a 96 well plate at ~5000 cells/well one day before transfection. USP36 siRNA-1 was transfected into the cells according to above protocol. Cell proliferation assay was performed 0, 24, 48 hours, and 72 hours after transfection using CellTiter 96R AQueous one solution Reagent (Promega G3580). 20 µl of the reagent was added into each well containing the samples, which were subsequently incubated at 37˚C for 1 hour in humidified, 5% CO_2 incubator. Absorbance at 490 nm was recorded using a 96 well plate reader. Background 490 nm absorbance was corrected by subtracting average 490 nm absorbance from no-cell control well.

RESULTS

Ubp10 regulates Rpa190 stability

Ubp10 regulates the ubiquitination state of Rpa190. First, we needed to determine if Rpa190 is ubiquitinated, and if that ubiquitination is regulated by Ubp10. To facilitate this, we added a C-terminal 3HA tag to Rpa190 expressed from its genomic locus in a strain that also expresses 8-histidine ubiquitin. We

then purified ubiquitinated proteins by metal affinity chromatography from full cell lysates of *UBP10* and *ubp10*Δ cells. The initial cell lysates showed us that Rpa190 protein levels are decreased approximately 5-fold in *ubp10*Δ cells than in *UBP10* cells (Figure 3.1, left panel). The *UBP10* lysate sample has been serial diluted for comparison to the *ubp10*Δ lysate. Conversely, the steady-state ubiquitination level of Rpa190 was approximately 4-fold higher in *ubp10*Δ cells, despite the lower total Rpa190 protein levels in these same cells (Figure 3.1, right panel). The *ubp10*Δ eluate has been serial diluted for comparison to the *UBP10* eluate. These results are consistent with Rpa190 being a substrate of Ubp10.

Ubp10 regulates the stability of Rpa190. The decreased steady-state protein level of Rpa190 in the *ubp10*Δ cells could be due to either an affect on the mRNA or on the protein. However, we showed previously by microarray analysis describing all the genes with altered transcription in *ubp10*Δ that *RPA190* transcription is increased by approximately 50% in *ubp10*Δ cells (Gardner et al., 2005b), thus the effect must be to regulation of the protein. To investigate this we did a cycloheximide-chase degradation assay following the abundance of Rpa190-3HA after the addition of the protein translation inhibitor in cells that were either *UBP10* or *ubp10*Δ. This experiment shows that Rpa190 is and stable in wild-type, *UBP10,* cells whereas in *ubp10*Δ cell, Rpa190 has a much lower steady-state level and was degraded over the course of three hours. This effect is directly due to loss of *UBP10* and not an additional mutation in the *ubp10*Δ

cells because the stability of Rpa190 was rescued by addition of *UBP10*. By contrast, addition of the catalytically inactive *ubp10*^{C371S} did not rescue the stability of Rpa190 (Figure 3.2), suggesting that the DUB activity of Ubp10 is required to stabilize RPA190. Rpa190 was stable in *sir2*Δ, *sir4*Δ and *ubp8*Δ cells (Figure 3.3), demonstrating that this effect on Rpa190 is not related to loss of rDNA silencing (*sir2*Δ), overall silencing or Ubp10 localization (*sir4*Δ), or general histone deubiquitination (*ubp8*Δ).

*Overexpression of Rpa190 rescues the ubp10*Δ *growth defect.* As we know that Ubp10's role in telomere silencing is not the cause of the *ubp10*Δ growth defect, we considered that it could be due to the drastically reduced levels of Rpa190. To test this, we overexpressed Rpa190 from a high copy plasmid in both *UBP10* and *ubp10*Δ cells (Figure 3.4). We found that by increasing the expression of Rpa190 we could rescue the slow growth phenotype in *ubp10*Δ cells. Overexpression of Rpa190 in *ubp10*Δ cells led to nearly equivalent amounts of Rpa190 being expressed in *UBP10* cells with normal Rpa190 levels (Figure 3.5). Thus, the loss of Ubp10's regulation of Rpa190 is sufficient to explain the growth defect in *ubp10*Δ cells.

The stability of RNA polymerase I is not nutrient sensitive, but is cold sensitive

Nutrient deprivation does not alter Rpa190 stability. Transcription of rDNA by RNAPI is tightly regulated to match production of ribosomes with cellular protein

synthesis needs (Russell and Zomerdijk, 2005). One of the primary conditions known to regulate RNAPI activity is nutrient availability. In particular, it was recently demonstrated that the stability of Rrn3, a transcription factor that recruits the RNAPI holoenzyme to the rDNA promoter (Yamamoto et al., 1996), is altered after TOR (Target of Rapamycin) inhibition by rapamycin or amino acid depletion from the growth media (Philippi et al., 2010). Therefore, we examined if Rpa190 stability in *UBP10* and *ubp10*Δ cells is altered upon rapamycin treatment, amino acid depletion, or glucose limitation. Under none of these conditions did we observe any effect on Rpa190 stability after these alterations (Figure 3.6). This is consistent with the previous observation that Rpa190 steady-state levels are unaffected after rapamycin treatment (Tsang et al., 2003). Thus, it appears that Rpa190 stability is not regulated by nutrient availability.

Rpa190 stability is cold sensitive. Interestingly, we found that the degradation of Rpa190 in *ubp10*Δ cells was dependent upon the growth temperature. As the growth temperature was increased, the stability of Rpa190 in *ubp10*Δ cells also increased (Figure 3.7, right panels). This correlated with the observation that the slow growth phenotype of *ubp10*Δ cells was progressively ameliorated when the cells were grown at increasingly higher temperatures (Figure 3.7, left panels). The cold sensitivity in growth of *ubp10*Δ cells has been noted previously (Amerik et al., 2000). Though it isn't clear why Rpa190 stability would be cold sensitive in *ubp10*Δ cells, it is known from *in vitro* studies that non-lethal defects in ribosome biogenesis result in cold-sensitive growth (Guthrie et al., 1969). We speculate

that ubiquitination of Rpa190 might serve as a checkpoint for a cold-sensitive step during rRNA transcription and Ubp10's function is to remove ubiquitin from Rpa190 once that checkpoint has been resolved.

Ubp10's regulation of RNA polymerase I stability is conserved in human USP36

USP36 rescues Rpa190 stability in yeast. The first experiment we did to see if USP36 was a functional ortholog of Ubp10 was to examine if it could complement the *ubp10*Δ phenotype in yeast. We placed USP36 behind the *UBP10* promoter in a yeast expression plasmid and transformed the plasmid into *ubp10*Δ cells. Expression of USP36 rescued Rpa190 stability to the level of *UBP10* (Figure 3.8), as shown by cycloheximide-chase degradation assay.

USP36 deubiquitinates Rpa190 in yeast. Next, we wanted to verify that the rescue of Rpa190 stability when USP36 is expressed is due to a decrease in ubiquitinated Rpa190. To do this, we transformed USP36 into the 8Xhistidine ubiquitin strains. After purifying the ubiquitinated proteins by metal affinity chromatography, we see that cells in which USP36 is expressed have nearly wild-type levels of ubiquitinated Rpa190 (Figure 3.9).

*Expression of USP36 can recover the ubp10*Δ *growth defect.* Lastly, since USP36 can rescue Rpa190 stability and ubiquitination level, we would expect it would also be able to recover the *ubp10*Δ growth defect. Serial dilution spot tests

show that USP36 expressed in *ubp10*Δ cells have a growth rate equivalent to *UBP10* cells (Figure 3.10).

Knockdown of USP36 in HeLa cells does not affect RPA194 mRNA levels. We next assessed if USP36 controls the levels of the largest subunit of RNAPI in human cells. To obtain knockdown of USP36, we transfected three different commercially available USP36 siRNA constructs (obtained from Applied Biosystems) into HeLa cells and, after 48 hours post-transfection, we observed an approximately 80% reduction in USP36 mRNA levels (Figure 3.11, left panel). Importantly, the knockdown of USP36 mRNA did not have an affect on the levels of RPA194 (the human homolog of yeast Rpa190), which coordinates with our data showing that *ubp10*Δ does not affect *RPA190* mRNA levels (Figure 3.11, right panel).

RPA194 levels decreased after USP36 knockdown. Correlating to the reduction in USP36 mRNA levels, 48 hours after transfection of the three USP36 siRNA, levels of USP36 protein were reduced by nearly 80% (Figure 3.12, middle row). At this time point we observed an approximately 50% decrease in the amount of RPA194 protein (Figure 3.12, top row), similar to the reduction of Rpa190 levels in the *ubp10*Δ cells in yeast. This reduction is specific to RPA194, as protein levels of the housekeeping gene GAPDH remained constant (Figure 3.12, bottom row).

USP36 knockdown causes proliferation defect in HeLa cells. When we examined the growth of USP36 siRNA-transfected cells, we found that they displayed reduced proliferation compared to mock-treated cells (Figure 3.13). This proliferation defect is akin to the growth rate defect seen in *ubp10*Δ cells in yeast. As reduction of USP36 in humans cells resulted in similar effects on RPA194 protein levels and cell growth as did reduction of Ubp10 levels in yeast cells on Rpa190, we conclude that regulation of the largest subunit through ubiquitination and deubiquitination is conserved in eukaryotes.

DISCUSSION

Prior to this research, the only known role for Ubp10 was the regulation of gene silencing at the telomeres by deubiquitination of histone H2B (Emre et al., 2005; Gardner et al., 2005b). Here, I have described a novel role for Ubp10 in the regulation of RNAPI ubiquitination and stability. We have also found that this is a conserved mechanism of regulation. Ubp10's human homolog, USP36, was able to functionally complement the *ubp10*Δ allele in yeast for RNAPI stability and growth, and performed an analogous function in human cells.

There is only one other known example where deubiquitination of the largest subunit of an RNA polymerase functions to control its stability. In budding yeast, the DUB Ubp3 regulates the ubiquitination and stability of Rpb1 (Kvint et al., 2008), the largest subunit of RNA polymerase II (RNAPII). Ubiquitination and Ubp3-mediated deubiquitination of Rpb1 is particularly pronounced under DNA damage conditions (Kvint et al., 2008), indicating that deubiquitination of RNAPII

is important in resolving damage-arrested RNAPII complexes. Furthermore, *ubp3*Δ cells are sensitive to the transcription elongation inhibitor 6-azauracil (Kvint et al., 2008), suggesting that Ubp3 may play a general role in the rescue of elongation-arrested RNAPII complexes. It has been proposed that Ubp3 surveys the ubiquitination status of RNAPII to prevent unwarranted destruction of an arrested RNAPII complex if the situation can be resolved (Kvint et al., 2008).

Although it appears that regulation of Ubp10-dependent Rpa190 stability is not controlled by nutrient availability, there are other possibilities for ubiquitin-mediated modulation of RNAPI function. For example, it could that Rpa190 is ubiquitinated and deubiquitinated to regulate a particular step in rDNA transcription such as initiation, elongation, termination, or reinitiation of transcription. Alternatively, RNAPI might be similarly ubiquitinated during elongation as RNAPII, and the role of Ubp10 would be analogous to Ubp3 – to rescue elongation-arrested RNAPI complexes. One intriguing observation that might hint at the latter possibility is the temperature dependence of RNAPI degradation in *ubp10*Δ cells (Figure 3.7). Ribosome assembly is inherently sensitive to low temperatures (Guthrie et al., 1969). It is possible that the assembling rRNA transcript has an increasing probability of becoming kinetically trapped in an unproductive folding intermediate at lower temperatures (Treiber and Williamson, 2001), which might lead to the arrest of the elongating RNAPI complex. Ubiquitination of the arrested RNAPI complex could serve as a timing mechanism for resolution of the rRNA kinetic trap. Ubp10's function in this regard would be to deubiquitinate RNAPI complexes once the trap has been resolved,

allowing the resolved RNAPI complex to proceed with transcription and ribosome assembly. At higher temperatures, kinetically trapped rRNA transcripts might be more easily resolved (or more easily avoided) due to increased free energy, and thus there would be fewer arrested RNAPI complexes requiring ubiquitination and deubiquitination.

Future work will be required to delineate where, when, and for what purpose Ubp10 regulates RNAPI stability. Importantly, it must be determined whether Ubp10's regulation of RNAPI is direct through deubiquitination of Rpa190 or indirect through the deubiquitination of another protein.

Abbreviations: RNAPI, RNA polymerase I; rRNA, ribosomal RNA; DUB, deubiquitinase; HA, hemagglutinin; mRNA, messanger RNA; rDNA, ribosomal DNA; TOR, target of rapamycin; siRNA, small interfering RNA; RNAPII, RNA polymerase II.

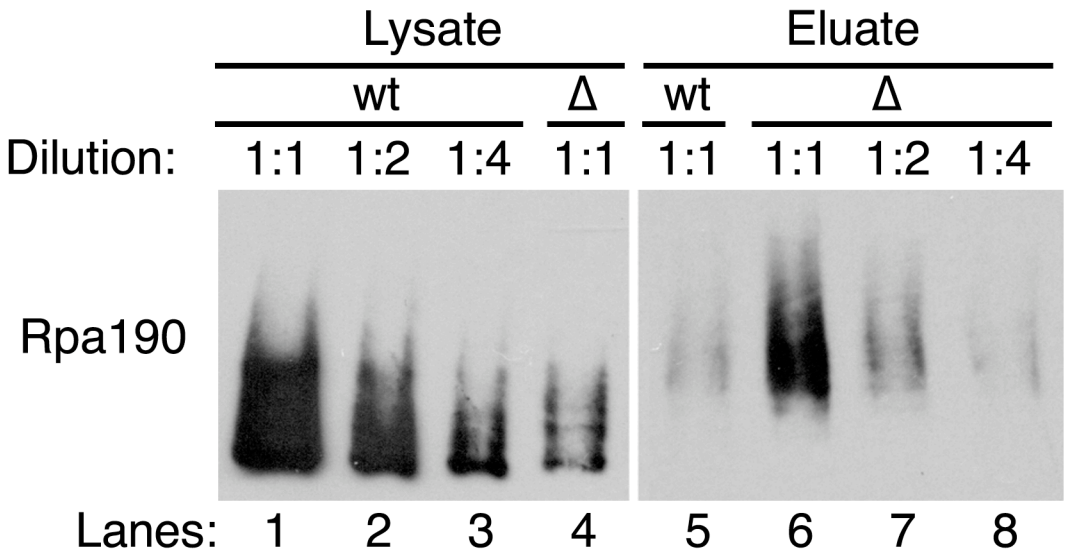

Figure 3.1: Ubp10 regulates the ubiquitination state of Rpa190. Ubiquitin proteomes from *UBP10* (wt) or *ubp10*Δ (Δ) cells were isolated by metal affinity purification. Levels of Rpa190-3HA in lysates (total protein) and eluates (ubiquitinated Rpa190) were determined by Western analysis using anti-HA antibodies. Lanes 1 and 4 indicate steady-state levels of Rpa190 in total lysates of *UBP10* and *ubp10*Δ cells. Lanes 5 and 6 show levels of ubiquitinated Rpa190 in the ubiquitin proteome of *UBP10* and *ubp10*Δ cells. Lanes 2 and 3 are 1:2 and 1:4 dilutions of the *UBP10* lysate sample. Lanes 7 and 8 are 1:2 and 1:4 dilutions of the *ubp10*Δ eluate sample.

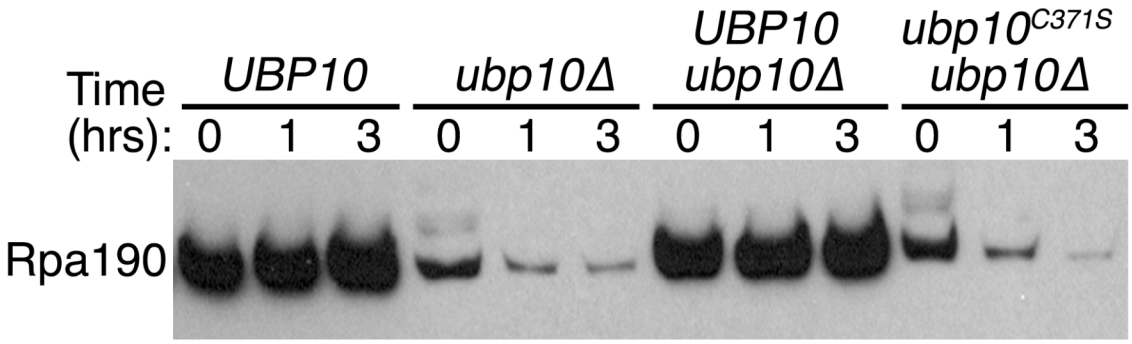

Figure 3.2: Ubp10 regulates the stability of Rpa190. Cycloheximide-chase degradation assays of *UBP10*, *ubp10*Δ, *UBP10-3HSV ubp10*Δ, or *ubp10*^{C371S}-*3HSV ubp10*Δ cells expressing Rpa190-3HA. Time after cycloheximide addition is indicated above each lane. Western analysis of whole cell extracts was performed using anti-HA antibodies.

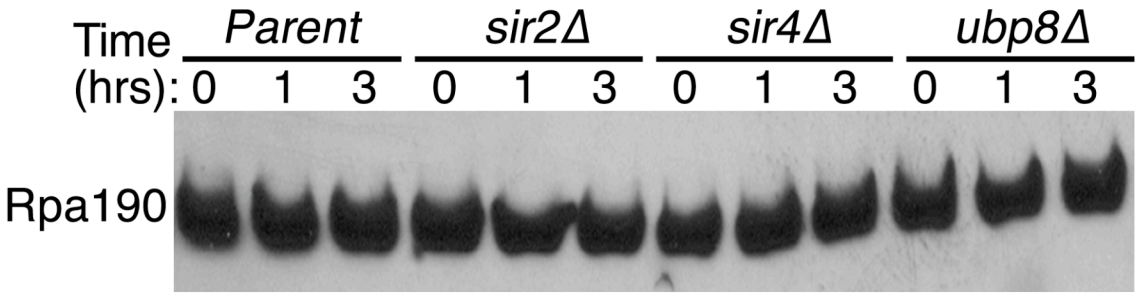

Figure 3.3: Rpa190 stability is not influenced by chromatin silencing or H2B deubiquitination. Cycloheximide-chase degradation assays of *UBP10*, *sir2*Δ, *sir4*Δ, or *ubp8*Δ cells expressing Rpa190-3HA. Time after cycloheximide addition is indicated above each lane. Western analysis of whole cell extracts was performed using anti-HA antibodies.

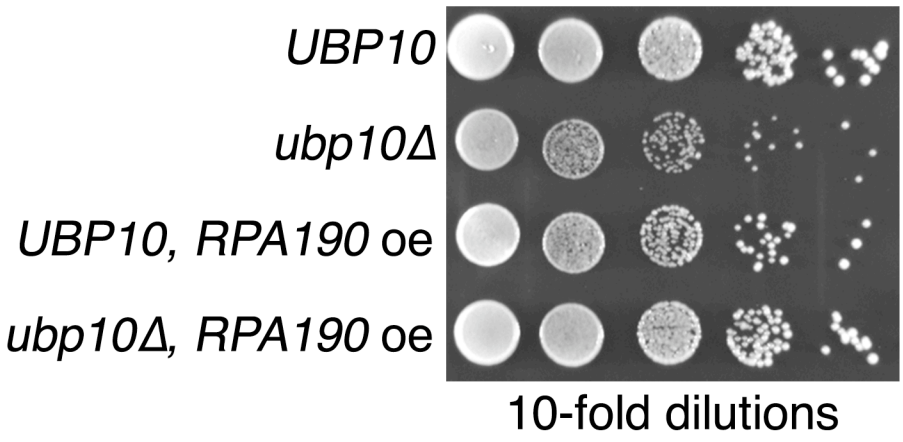

Figure 3.4: Overexpression of Rpa190 rescues the *ubp10*△ growth defect. Growth of *UBP10* and *ubp10*△ cells with or without *RPA190* overexpression (oe). 10-fold serial dilutions of cells were spotted onto the appropriate media and incubated at 30˚C for 3 days.

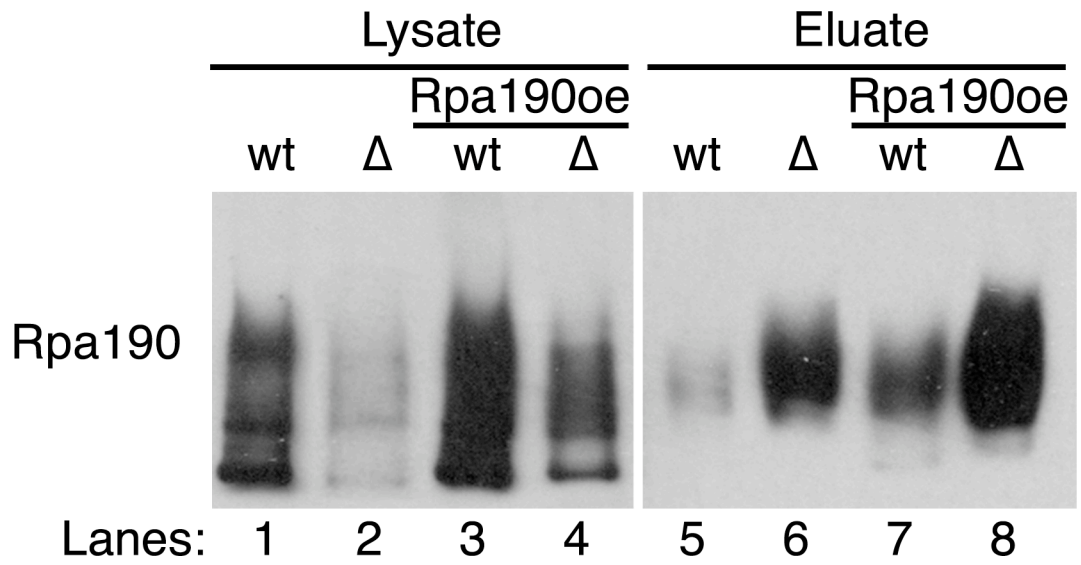

Figure 3.5: Wild-type Rpa190 levels restored in *ubp10*Δ cells by overexpression of Rpa190. Ubiquitin proteome analysis from *UBP10* (wt) or *ubp10*Δ (Δ) cells overexpressing (oe) Rpa190 were isolated by metal affinity purification. Levels of Rpa190-3HA in lysates (total protein) and eluates (ubiquitinated Rpa190) were determined by Western analysis using anti-HA antibodies.

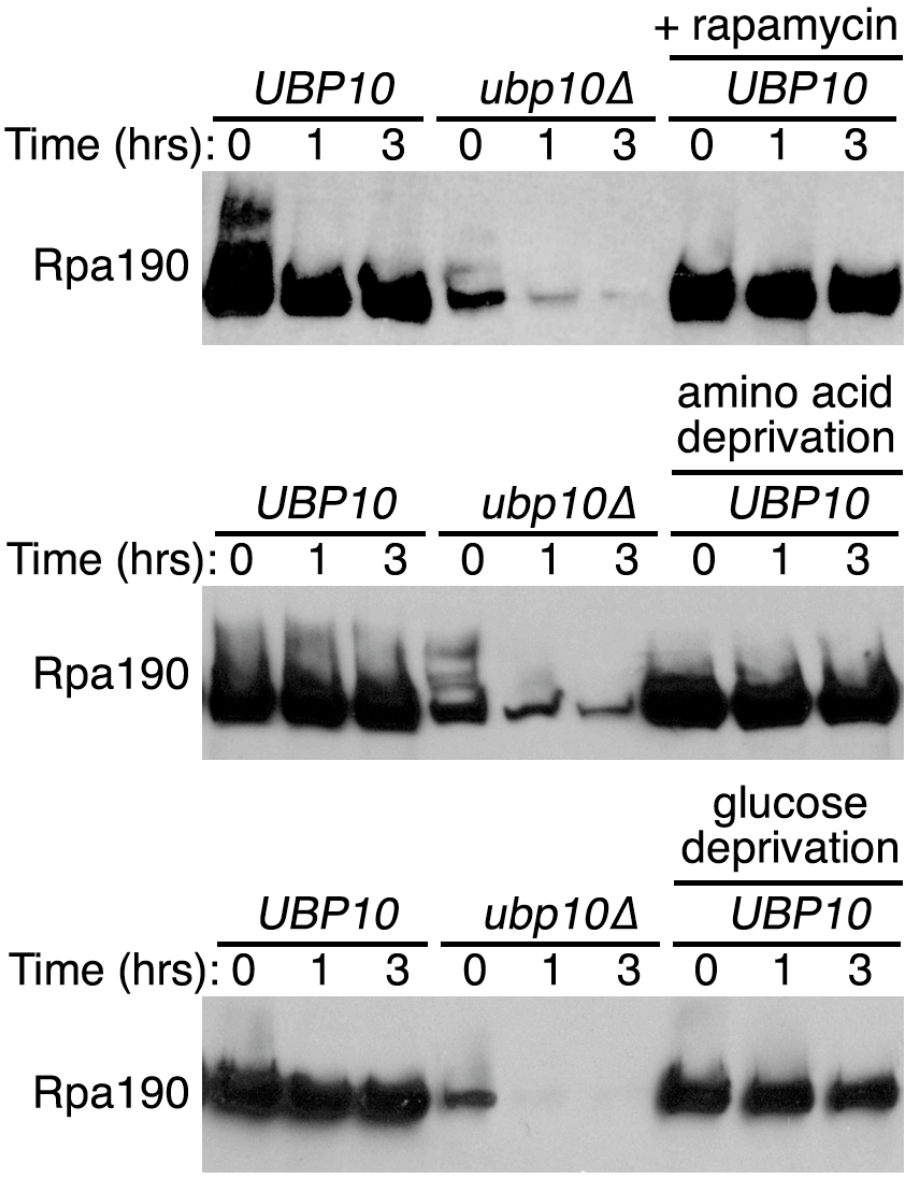

Figure 3.6: Rpa190 stability is not nutrient sensitive. Cycloheximide-chase degradation assays of *UBP10* and *ubp10*Δ cells expressing Rpa190-3HA. Cultures were grown in YPD then shifted to YPD + 200nM rapamcyin, YC, YC – tryptophan, or YP – glucose for two hours before the addition of cycloheximide. Time after cycloheximide addition is indicated above each lane. Western analysis of whole cell extracts was performed using anti-HA antibodies.

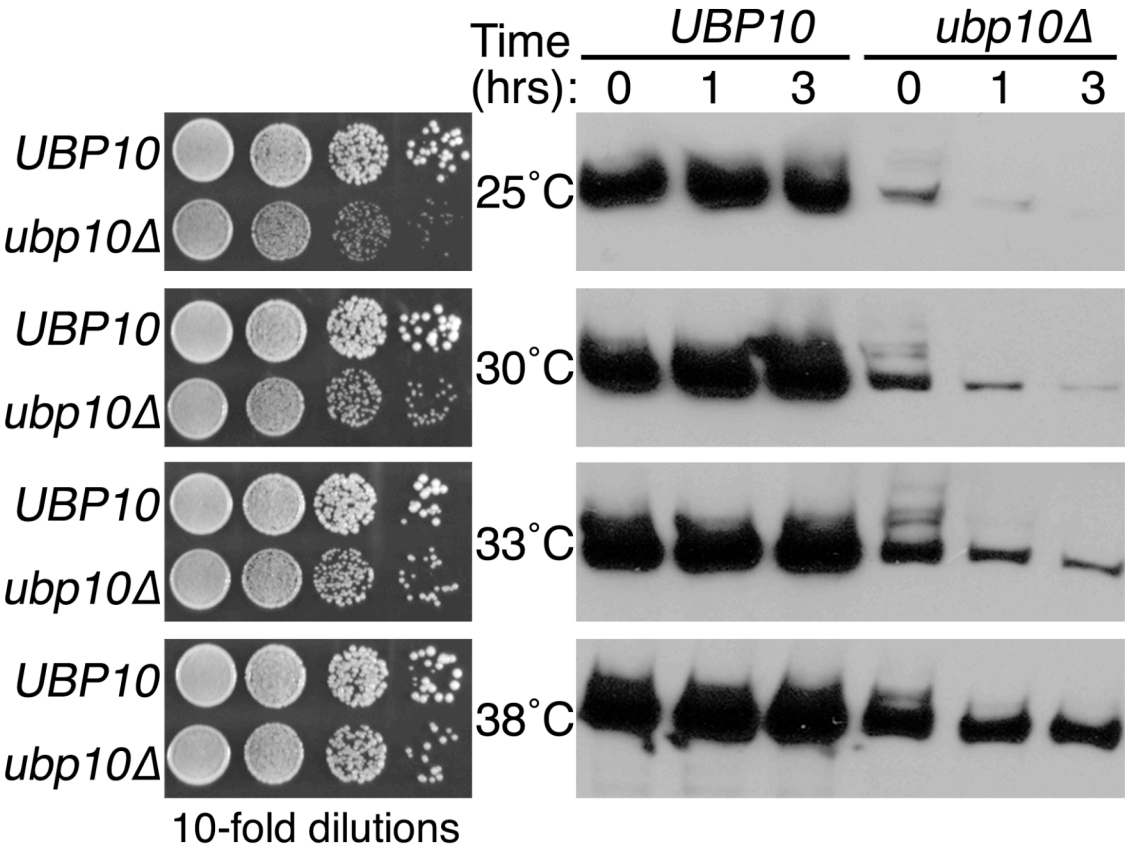

Figure 3.7: Rpa190 stability is cold sensitive. Growth of *UBP10* and *ubp10*Δ cells (left panels). 10-fold serial dilutions of cells were spotted onto the appropriate media and incubated at the indicated temperature for 3 days (30˚C, 33˚C, or 38˚C) or 5 days (25˚C). Cycloheximide-chase degradation assays of *UBP10* or *ubp10*Δ cells expressing Rpa190-3HA (right panels). Cells were grown at the indicated temperature. Time after cycloheximide addition is indicated above each lane. Western analysis was performed using anti-HA antibodies.

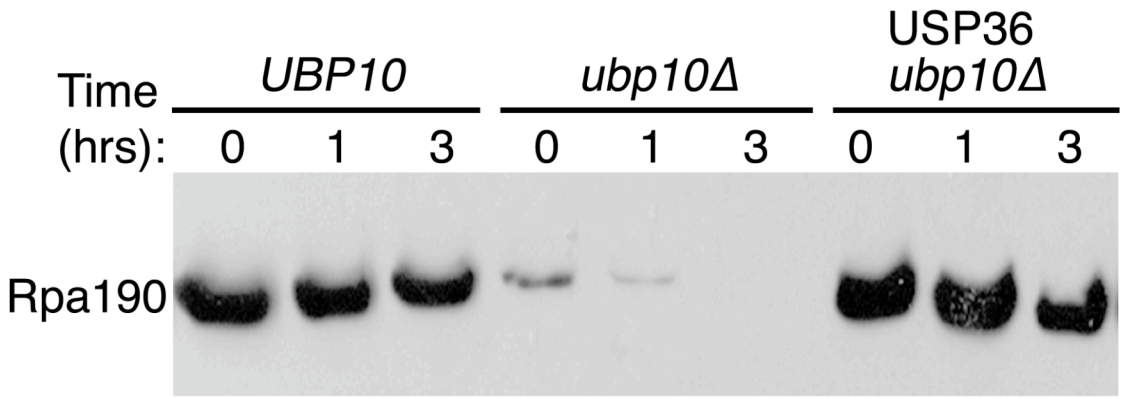

Figure 3.8: USP36 rescues Rpa190 stability in yeast. Cycloheximide-chase degradation assays of *UBP10*, *ubp10*Δ, or *USP36 ubp10*Δ cells expressing Rpa190-3HA. Time after cycloheximide addition is indicated above each lane. Western analysis of whole cell extracts was performed using anti-HA antibodies.

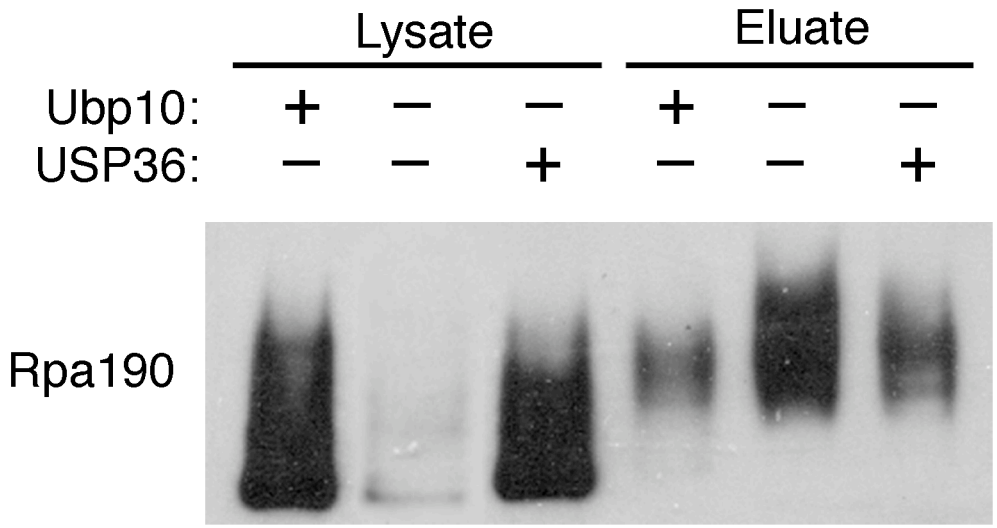

Figure 3.9: USP36 deubiquitinates Rpa190 in yeast. Ubiquitin proteomes from *UBP10*, *ubp10*Δ, or *USP36 ubp10*Δ cells were isolated by metal affinity purification. Levels of Rpa190-3HA in lysates (total protein) and eluates (ubiquitinated Rpa190) were determined by Western analysis using anti-HA antibodies.

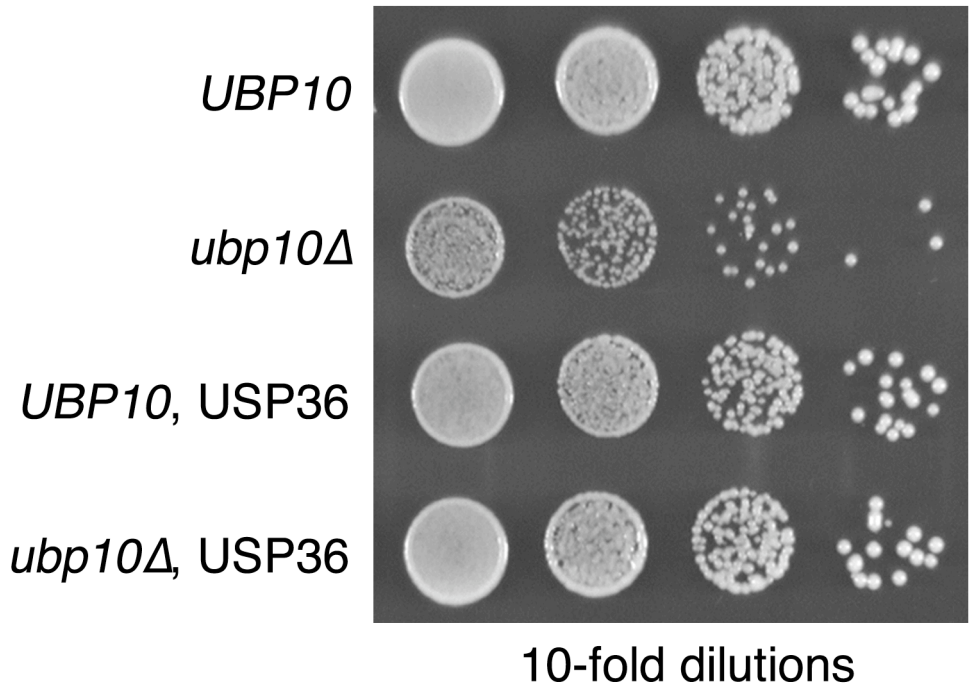

Figure 3.10: Expression of USP36 can recover the ubp10Δ growth defect. Growth of *UBP10* and *ubp10*Δ cells with or without USP36. 10-fold serial dilutions of cells were spotted onto the appropriate media and incubated at 30˚C for 3 days.

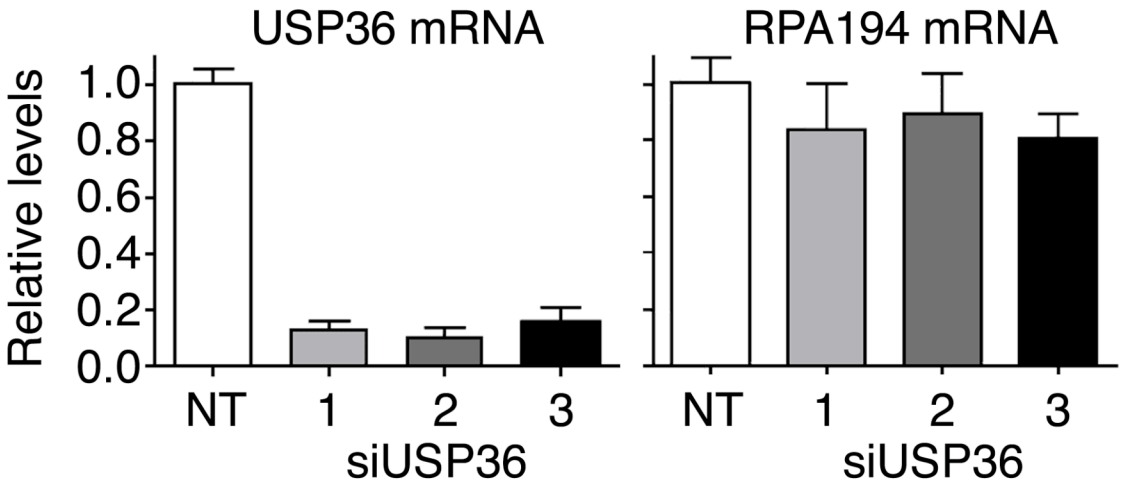

Figure 3.11: Knockdown of USP36 in HeLa cells does not affect RPA194 mRNA levels. HeLa cells were transfected with a non-targeting siRNA (NT) or three independent USP36 siRNAs (1, 2, or 3) for 48 hours. Relative USP36 (left panel) and RPA194 (right panel) mRNA levels were determined by RT-PCR after transfection. Data represent the average of 3 independent experiments, each performed in duplicate.

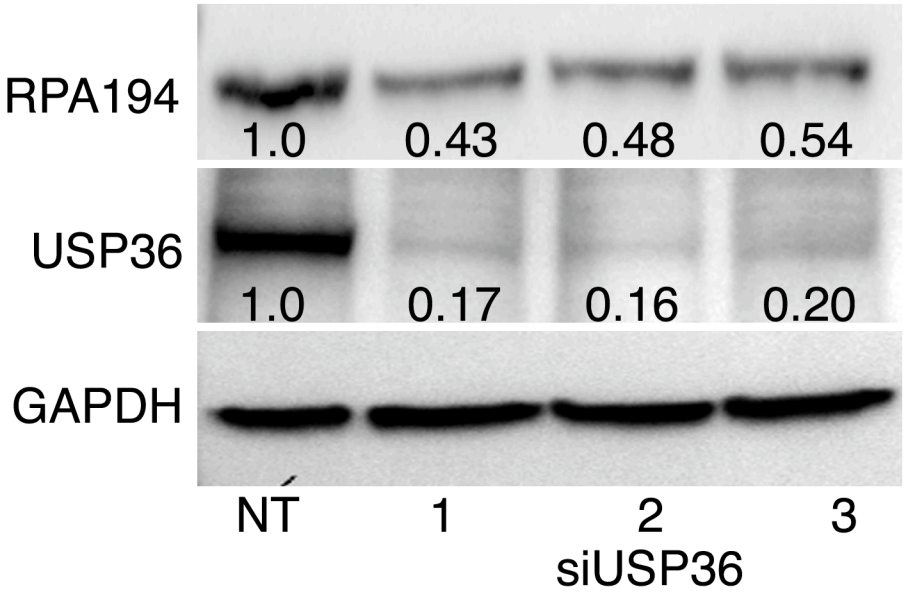

Figure 3.12: RPA194 levels decreased after USP36 knockdown. HeLa cells were transfected with non-targeting siRNA (NT) or three independent USP36 siRNAs (1, 2, or 3) for 48 hours. Western analysis of whole cell extracts at 48 hours post-transfection was performed using anti-RPA194 (top panel), anti-USP36 (middle panel), or anti-GAPDH (bottom panel) antibodies. ImageJ was used to measure signal intensity of each band. Numbers in each lane represent RPA194 and USP36 levels that were normalized using GAPDH and quantitated against the levels in the non-targeting siRNA (NT) lane.

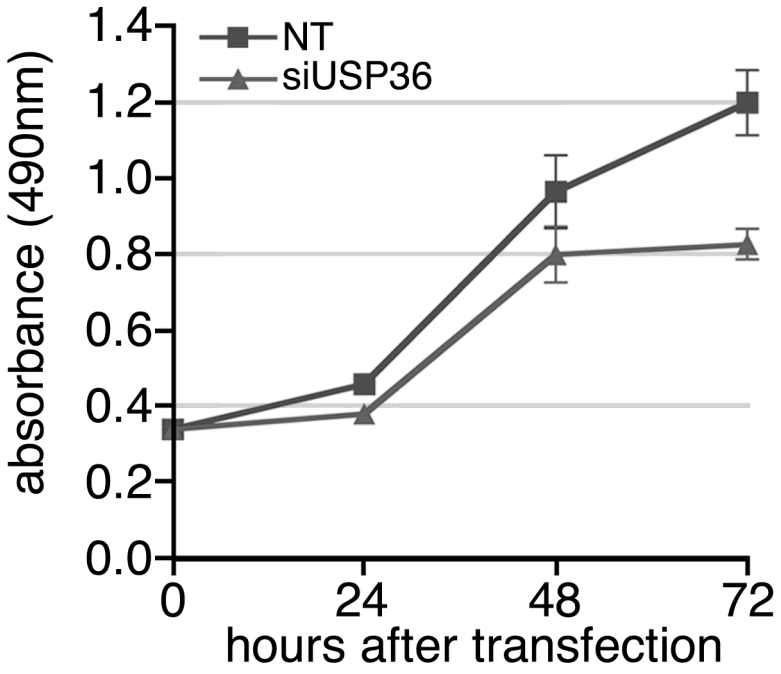

Figure 3.13: USP36 knockdown causes proliferation defect in HeLa cells. Defect in HeLa cell proliferation with siUSP36 treatment. HeLa cells were transfected with siUSP36-1 and a cell proliferation assay was performed at 0, 24, 48 and 72 hours after transfection. Cell proliferation was measured as absorbance at 490nm. The data represent 2 independent experiments with triplicates for each experiment at each time point.

CHAPTER IV: OTHER NUCLEOLAR ROLES OF UBP10

INTRODUCTION

The role for Ubp10 in the regulation of stability of RNAPI appears to be just one aspect of Ubp10 function in the nucleolus. Our proteomic analysis revealed Ubp10 interacting with numerous proteins and subcomplexes involved in ribosome biogenesis. However, the functional reason for these interactions is unclear. Ubp10 appears to interact with two classes of proteins: components of the small subunit (SSU) processome and proteins involved in the modification of pre-rRNA molecules. The SSU processome is a large, macromolecular complex that facilitates many important steps in ribosome biogenesis, including 35S transcription, cleavage, and proper rRNA folding (Phipps et al., 2011). Modification of bases in the rRNA, by 2'-O-methylation and pseudouridylation, are also critical to the folding of the rRNA as well as its activity in the ribosome (Decatur and Fournier, 2002). Both of these processes are critical to ribosome biogenesis, yet their mechanisms of regulation are virtually unknown.

MATERIALS AND METHODS

Yeast strains and plasmids. All yeast strains and plasmids are described in Appendix I. Standard yeast genetic methods were used in these studies (Guthrie and Fink, 1991).

Nondenaturing coimmunoprecipitation. Cultures were grown to ~1.8x10^7 cells/ml. Harvested cells were lysed in IP buffer. Lysates were diluted 1:5 in IP buffer and incubated for 16 hours at 4˚C with 1:1000 mouse anti-HSV antibody (Novagen) bound to 1.25 mg/ml Protein A Dynabeads (Invitrogen). Beads were washed three times in IP buffer. Proteins were eluted by incubation at 65˚C for 10 minutes in SUMEB (SUME + 0.01% bromophenol blue). Proteins were separated on 8% SDS-PAGE gels, transferred to nitrocellulose, and visualized with anti-HSV (Novagen) or anti-HA (Sigma) antibodies.

Cycloheximide-chase degradation assays. Cycloheximide-chase degradation assays were performed similar to previously described (Gardner et al., 2005a). Cultures were grown to a cell density of 1x10^7 cells/ml. Cycloheximide was added to a final concentration of 50 µg/ml and the cells were further incubated at 30°C for 0–3 hours. Cells were lysed at the appropriate time point in 200 µl SUMEB with 10 mM PMSF. Proteins were separated on 8% SDS-PAGE gels, transferred to nitrocellulose, and visualized with anti-HA (Sigma) antibodies.

RESULTS

Ubp10 interacts and modulates nucleolar proteins

Ubp10 forms a stable interaction with numerous nucleolar proteins. Of the thirty-seven nucleolar proteins that we found to interact with Ubp10 in the crosslinking analysis, we chose fifteen to verify by traditional coIP or yeast 2-hybrid (Y2H) assay. These techniques require a stable interaction between Ubp10 and the

target protein, as there is no crosslinking agent to maintain the interaction. To facilitate the coIP, we added a 3HA tag to the C-terminus of the Ubp10-interacting proteins in a strain expressing Ubp10-3HSV. For the Y2H, we tested if a Gal4 binding domain (GBD) fusion to Ubp10 could interact with Gal4 activation domain (GAD) fusions of the target proteins. Of the fifteen, six retested as positive interactors: four were verified by coIP (Cbf5, Nop56, Nop58, and Pwp2), and two were verified with Y2H (Dhr2 and Utp22). Thus, some of the interacting proteins identified by crosslinking coIP MS/MS form stable interactions with Ubp10.

Ubp10 modulates the stability of nucleolar proteins. Using a standard cycloheximide-chase degradation assay, we also assessed if deletion of *UBP10* led to a change in stability of any of the proteins that we identified in our crosslinking screen. We identified seven proteins (not including Rpa190) that in *ubp10*Δ cells showed increased degradation compared to in *UBP10* cells. These proteins are: Cbf5, Nop56, Nop58, Pwp2, Utp22, Rrp5, and Mpp10. Interestingly, five of these seven proteins were also identified as forming a stable interaction with Ubp10.

DISCUSSION

Does Ubp10 regulate the SSU processome?

The SSU processome is a ribonucleoprotein (RNP) complex that is composed of several distinct subcomplexes. The essential function of the SSU

processome is to aid in the cleavage at sites A_0, A_1, and A_2, which are the cleavage events that liberate the 18S rRNA from the 35S rRNA (Phipps et al., 2011). These cleavage steps are dependent on the U3 small nucleolar RNA (snoRNA), which has regions of complementarity to the rRNA that are thought to act as a molecular guide (Mereau et al., 1997). One of the key components of the SSU processome is the UTP-A complex, which is important for both the transcription of the pre-rRNA and its processing (Bernstein et al., 2004; Dragon et al., 2002). Ubp10 was identified as interacting with four proteins in the UTP-A complex (Pol5, Utp10, Utp17 and Utp4) in our crosslinking screen. It is thought that association of the UTP-A complex to the nascent pre-rRNA aids in the initiation and processivity of RNAPI (Bernstein et al., 2004; Dragon et al., 2002). As we have shown that Ubp10 regulates the ubiquitination state of RNAPI, it may be that the UTP-A complex is localizing Ubp10 to the polymerase during this critical step in transcription to deubiquitinate it. This would be akin to how Sir4 guides Ubp10 to the silent telomeres for its function there (Gardner et al., 2005b). Ubp10 may also be acting on members of the UTP-A complex itself to manage their stability or activity. The association of Ubp10 with the UTP-A complex may also help explain the temperature dependence of RNAPI stability. Since UTP-A is required for efficient transcription, the absence of Ubp10 may prevent the assembly of the UTP-A/RNAPI complex, which could cause the polymerase to stall, leading it to be ubiquitinated. Again, without Ubp10, this ubiquitination cannot be resolved, and the polymerase would be degraded. However, at

increased temperature, the increased free energy may help overcome the need for deubiquitination by Ubp10.

Ubp10 also interacts with proteins of the UTP-B and UTP-C subcomplexes. The exact molecular functions of these groups are not known at this time, but they are essential for the proper processing of the 18S rRNA. Ubp10 forms stable interactions with members of these two subcomplexes, through Pwp2 and Utp22, and in the absence of *UBP10,* they have an increased rate of degradation. This suggests that Ubp10 may have a role in the processing of the 18S rRNA. Interestingly, other high-throughput proteomic analyses in budding yeast (Krogan et al., 2006), human cells (Sowa et al., 2009), and fission yeast (Kouranti et al., 2010) found that Ubp10 and its orthologs (USP36 in humans, Ubp16 in fission yeast) interact with some of the same ribosome biogenesis factors that we identified in our study, suggesting that this mechanism of regulation is conserved through evolution.

Is Ubp10 a regulator of rRNA modification?

Ribose-2'-O-methylation and pseudouridylation are primary post-transcriptional modifications of the 18S and 25S rRNAs mediated by Box C/D snoRNPs and Box H/ACA snoRNPs, respectively. While most modifications are not essential, they are thought to contribute small benefits to ribosome function, possibly by refining rRNA structure (Decatur and Fournier, 2002). Altered bases can lead to changes in the structure of the RNA, allowing for different hydrogen-bond formation, increased local bases stacking, and more structural rigidity

(Decatur and Fournier, 2002). The main protein constituents in the yeast Box C/D snoRNP are Nop1/fibrillarin, Nop56, Nop58, and Snu13 (Watkins et al., 2000). We found both Nop56 and Nop58 interact with Ubp10, as well as have decreased stability in *ubp10*Δ cells. Box H/ACA snoRNP is composed of Cbf5, Gar1, Nhp2, and Nop10 in yeast (Meier, 2005). Cbf5 has a stable interaction with Ubp10, and is also degraded in the absence of *UBP10*, suggesting that Ubp10 may regulate both of these mechanisms of rRNA modification.

The effect that altering rRNA modification could have on cells is not entirely clear at this point, however since these modifications tend to cluster in highly conserved, functional, regions of the ribosome, it implies that these modifications influence both the structure and function of the ribosome (Lane et al., 1995). It is known that these modifications can influence protein translation efficiency (Raue et al., 1988). Additionally, alterations in the pseudouridylation machinery can lead to a selective problem in the translation of mRNAs containing internal ribosome entry site elements (Yoon et al., 2006). In this way, Ubp10 would exert control on protein synthesis by two mechanisms of regulation: first, the creation of ribosomes, by affecting RNAPI stability, and second, protein translation efficiency, by RNA modification alteration, making Ubp10 a critical cell regulator.

Abbreviations: SSU, small subunit; coIP, coimmunoprecipitation; Y2H, yeast 2-hybrid; GBD, Gal4 binding domain; GAD, Gal4 activation domain; RNP, ribonucleolprotein; snoRNA, small nucleolar RNA; rRNA, ribosomal RNA; RNAPI, RNA polymerase I; snoRNP, small nucleolar ribonucleolprotein; mRNA, messanger RNA.

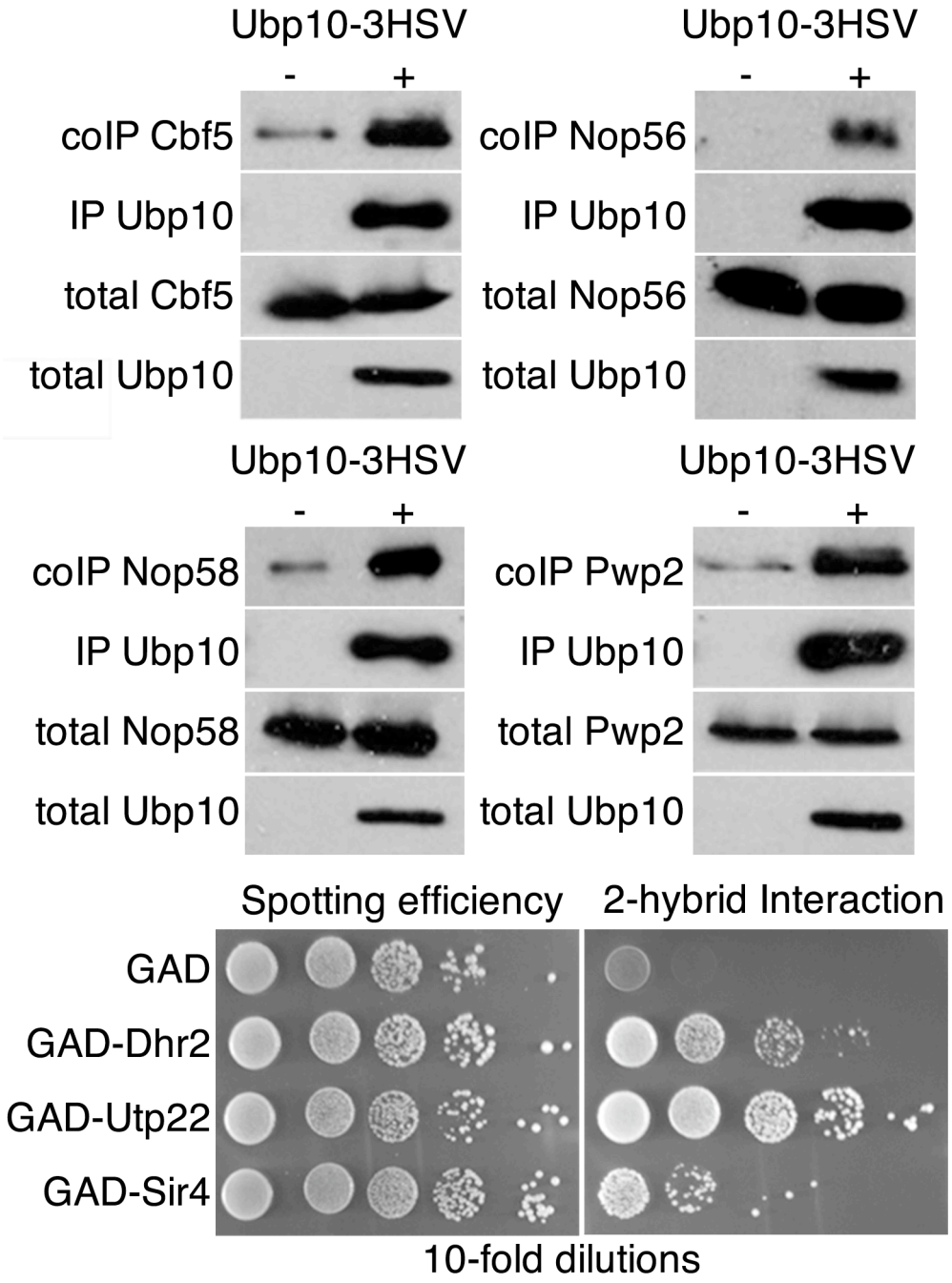

Figure 4.1: Ubp10 forms stable interactions with nucleolar proteins. (a) coIPs between Ubp10-3HSV and the indicated 3HA-tagged target proteins. Ubp10-3HSV was purified with its interacting proteins by immunoprecipitation using anti-HSV antibodies. Lysates and coIPs were analyzed by anti-HSV and anti-HA western blotting. (**b**) Yeast 2-hybrid (Y2H) interactions between cells expressing GBD-Ubp10 and each indicated GAD fusion protein. Cells were spotted onto media plus or minus histidine to measure spotting efficiency and Y2H interaction, respectively.

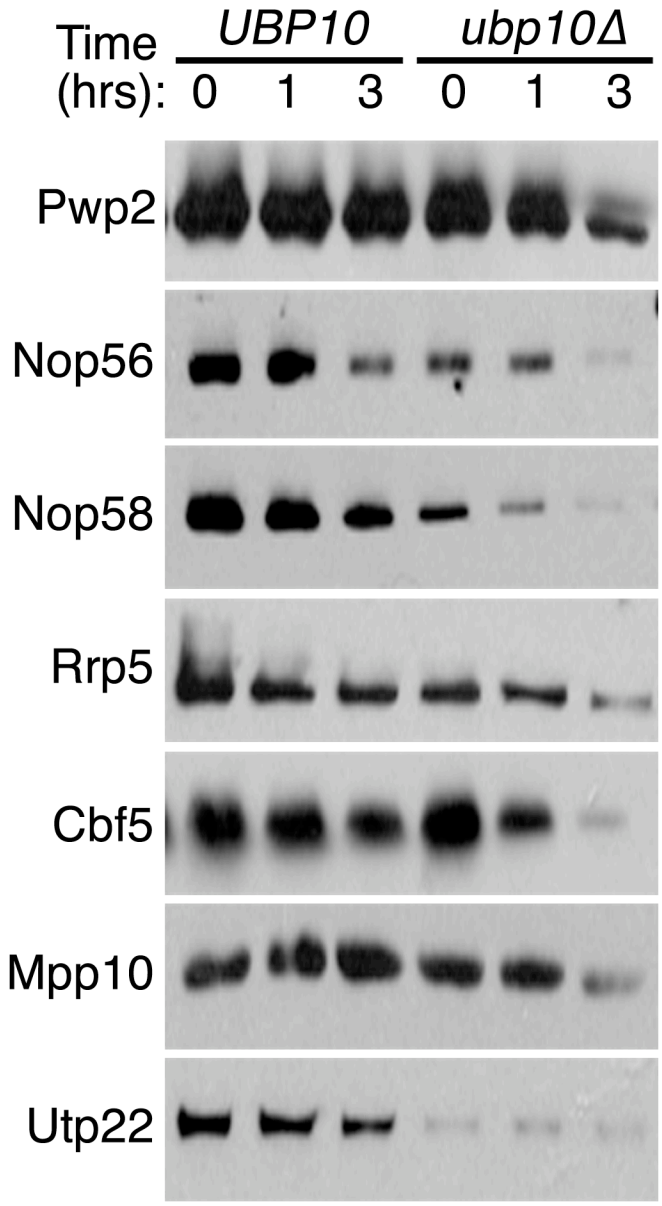

Figure 4.2: Ubp10 interacting proteins have decreased stability in the absence of *UBP10.* Cycloheximide-chase degradation assays of *UBP10* and *ubp10*Δ cells expressing 3HA-tagged Ubp10 interacting proteins. Time after cycloheximide addition is indicated above each lane. Western analysis of whole cell extracts was performed using anti-HA antibodies.

CHAPTER FIVE: CONCLUSIONS

The research that I have conducted for my doctoral dissertation has elucidated a novel role for the yeast deubiquitinase Ubp10. I have shown that Ubp10 is predominately localized to the nucleolus, where it likely performs several functions. *ubp10*Δ cells have a significant reduction in pre-rRNAs, mature rRNAs and translating ribosomes. Proteomic analysis revealed extensive interactions between Ubp10 and the ribosome biogenesis machinery, as well as identified a new substrate for Ubp10. Rpa190, the largest subunit of RNA polymerase I (RNAPI), is stabilized via Ubp10-dependent deubiquitination, and this is required to achieve optimal ribosome content and cell growth.

One aspect of Ubp10 biology that has yet to be elucidated is its potential role in metabolic regulation. The growth defect seen in *ubp10*Δ cells is exacerbated when combined with mutations in the nutrient biosynthetic pathway (Kahana and Gottschling, 1999), suggesting Ubp10 may be involved in the regulation of nutrient transport or utilization. Kahana et al., 2001 demonstrated that the general amino acid permease Gap1 has reduced protein levels and activity in *ubp10*Δ cells. In addition to this, my proteomic data reveals further evidence that Ubp10 is involved in these nutrient-related pathways. From the crosslinking proteomics, we identified several enzymes involved in lysine (Lys20) and uracil (Ura2, Ura5, and Ura7) biosynthesis. Importantly, these include the rate-limiting enzymes in these pathways, further highlighting the possible significance of this potential regulation by Ubp10.

Ubp10 is a fascinating enzyme in that it is involved in the regulation of at least two disparate cellular processes, ribosome biogenesis and telomeric silencing. An interesting question is then raised as to why these processes are linked through this one enzyme. One hypothesis is related to cell stress response. Under conditions of cell stress, Sir3 is phosphorylated, leading to a decreased in subtelomeric silencing and an increased in transcription of subtelomeric genes (Ai et al., 2002). According to Orlandi et al, 2004, the transcription profile of *ubp10*Δ cells closely resembles that of a cell undergoing oxidative stress. They also observed an increase in reactive oxygen species and DNA fragmentation in *ubp10*Δ cells, which are markers of apoptosis (Orlandi et al., 2004). This suggests that the regulation of gene expression by Ubp10 may link stress response and silencing. It is well established that the stress response also affects ribosome biogenesis. Ribosome biogenesis is down regulated under condition of nutrient limitation, high cell density, translation and TOR inhibition. In human cells, the predominately cellular surveillance mechanism is through the p53-MDM2 pathway. p53-MDM2 is activated under numerous conditions, including inhibition of rRNA synthesis (Sun et al., 2007), disruption of rRNA processing (Pestov et al., 2001), and imbalance of ribosomal proteins (Lindstrom and Zhang, 2008). With the exception of the latter, we have shown Ubp10/USP36 to affect these processes (Figure 2.4 and 2.6), thus creating an axis of regulation where the cell can regulate both subtelomeric gene expression and ribosome biogenesis by the control of one enzyme.

Aberrant ribosome biogenesis has long been linked to cancer. Both morphological and functional changes in the nucleolus are widely observed in cancer tissues, due to the increased demand for ribosomes in proliferating cells (Derenzini and Ploton, 1991). As a regulator of ribosome biogenesis, Ubp10 may have an oncogenic potential. For example, Ubp10 has been identified as an interactor with Cbf5 and Gar1, two of the core subunits of the snoRNP complex responsible for most of the pseudouridylation of rRNA (Wang et al., 2002). The human homologue of Cbf5 is dyskerin, which when mutated, leads to a rare inherited syndrome called X-linked dyskeratosis congenita (DC). DC is characterized by skin, mucosal and bone marrow failure, as well as an increased risk of tumor development (Dokal, 2000). The mutation in dyskerin that leads to DC causes a decreased rate of pseudouridylation, and thus a decreased rate of rRNA processing (Ruggero et al., 2003). The mechanism for DC pathogenesis is unique, the defect in pseudouridylation leads to a selective problem in the translation of a group of mRNAs containing internal ribosome entry site elements. These mRNAs included several encoding tumor suppressors, such as p27, Bcl-xL and XIAP, which at least partially explains the neoplastic phenotype (Yoon et al., 2006). By the regulation of Cbf5, Ubp10 may have the potential to mediate such processes. Other diseases, including Diamond-Blackfan anemia and cartilage-hair hypoplasia, are characterized by ribosome biogenesis dysfunction. These diseases are also linked to an increased susceptibility to cancer development, which may be due to the induction, then selective loss, of the ribosomal protein-Mdm2-p53 response (reviewed in (Deisenroth and Zhang)).

This indicates that the regulation of the ribosome biogenesis pathway by Ubp10/USP36 could be critical in the prevention of the activation of the p53 pathway, and thus the induction of carcinogenesis.

I have identified that USP36, the human homolog of Ubp10, regulates RNAPI in an analogous fashion in human cells. Importantly, USP36 shows increased expression in ovarian cancer cells (Li et al., 2008). In a similar mechanism to the Ubp10 regulation of cell growth in yeast, USP36 is important for cell proliferation *in vitro* (Figure 3.13 and (Endo et al., 2009)), and the *Drosophila* homolog scrawny is important for stem cell proliferation *in vivo* (Buszczak et al., 2009), it is conceivable that cells with high proliferative capacity like cancer cells require increased levels of USP36 to achieve the elevated levels of RNAPI and ribosome production required for rapid proliferation. This possibility is especially salient when framed against the growing body of literature implicating upregulation of ribosome biogenesis as a key factor in tumorigenesis (Montanaro et al., 2008). USP36 has also been shown to regulate the stability of the nucleolar protein nucleophosmin/B23 (NPM) (Endo et al., 2009) in human cells. NPM is an endoribonuclease that cleaves the 32S pre-rRNA to liberate the 28S mature rRNA (Savkur and Olson, 1998) and also regulates the p53 checkpoint by its direct association with Arf (ADP ribosylation factor) (Korgaonkar et al., 2005). Mutations of the *NPM* gene have a frequent association with human cancer (Grisendi et al., 2006). Thus, by stabilizing NPM, USP36 contributes to the regulation of the p53 checkpoint. More studies will be needed

to assess if USP36 has true oncogenic potential due its regulation of RNAPI stability and/or some other critical step in ribosome biogenesis.

Abbreviations: rRNA, ribosomal RNA; TOR, target of rapamycin; DC, X-linked dyskeratosis congenita; NPM, nucleophosmin/B23; Arf, ADP ribosylation factor.

References

Ai, W., Bertram, P.G., Tsang, C.K., Chan, T.F., and Zheng, X.F. (2002). Regulation of subtelomeric silencing during stress response. Mol Cell *10*, 1295-1305.

Amerik, A.Y., and Hochstrasser, M. (2004). Mechanism and function of deubiquitinating enzymes. Biochim Biophys Acta *1695*, 189-207.

Amerik, A.Y., Li, S.J., and Hochstrasser, M. (2000). Analysis of the deubiquitinating enzymes of the yeast Saccharomyces cerevisiae. Biol Chem *381*, 981-992.

Aparicio, O.M., Billington, B.L., and Gottschling, D.E. (1991). Modifiers of position effect are shared between telomeric and silent mating-type loci in S. cerevisiae. Cell *66*, 1279-1287.

Ardley, H.C., Scott, G.B., Rose, S.A., Tan, N.G., and Robinson, P.A. (2004). UCH-L1 aggresome formation in response to proteasome impairment indicates a role in inclusion formation in Parkinson's disease. J Neurochem *90*, 379-391.

Barriere, H., Nemes, C., Du, K., and Lukacs, G.L. (2007). Plasticity of polyubiquitin recognition as lysosomal targeting signals by the endosomal sorting machinery. Mol Biol Cell *18*, 3952-3965.

Bernstein, K.A., Gallagher, J.E., Mitchell, B.M., Granneman, S., and Baserga, S.J. (2004). The small-subunit processome is a ribosome assembly intermediate. Eukaryot Cell *3*, 1619-1626.

Brachmann, C.B., Davies, A., Cost, G.J., Caputo, E., Li, J., Hieter, P., and Boeke, J.D. (1998). Designer deletion strains derived from Saccharomyces

cerevisiae S288C: a useful set of strains and plasmids for PCR-mediated gene disruption and other applications. Yeast *14*, 115-132.

Buszczak, M., Paterno, S., and Spradling, A.C. (2009). Drosophila stem cells share a common requirement for the histone H2B ubiquitin protease scrawny. Science *323*, 248-251.

Chau, V., Tobias, J.W., Bachmair, A., Marriott, D., Ecker, D.J., Gonda, D.K., and Varshavsky, A. (1989). A multiubiquitin chain is confined to specific lysine in a targeted short-lived protein. Science *243*, 1576-1583.

Chenon, M., Camborde, L., Cheminant, S., and Jupin, I. (2011). A viral deubiquitylating enzyme targets viral RNA-dependent RNA polymerase and affects viral infectivity. Embo J *31*, 741-753.

Ciechanover, A. (2006). The ubiquitin proteolytic system: from a vague idea, through basic mechanisms, and onto human diseases and drug targeting. Neurology *66*, S7-19.

Collart, M.A., and Oliviero, S. (1994). Preparation of yeast RNA. In Current Protocols in Molecular Biology, F.M. Ausubel, R. Brent, R.E. Kingston, D.D. Moore, J.G. Seidman, J.A. Smith, and K. Struhl, eds. (New York, John Wiley & Sons, Inc), pp. 13.12.11-13.12.12.

Colomer Gould, V.F. (2005). Mouse models of Machado-Joseph disease and other polyglutamine spinocerebellar ataxias. NeuroRx *2*, 480-483.

Craig, R., and Beavis, R.C. (2004). TANDEM: matching proteins with tandem mass spectra. Bioinformatics *20*, 1466-1467.

Das, C., Hoang, Q.Q., Kreinbring, C.A., Luchansky, S.J., Meray, R.K., Ray, S.S., Lansbury, P.T., Ringe, D., and Petsko, G.A. (2006). Structural basis for conformational plasticity of the Parkinson's disease-associated ubiquitin hydrolase UCH-L1. Proc Natl Acad Sci U S A *103*, 4675-4680.

Decatur, W.A., and Fournier, M.J. (2002). rRNA modifications and ribosome function. Trends Biochem Sci *27*, 344-351.

Deisenroth, C., and Zhang, Y. (2010). Ribosome biogenesis surveillance: probing the ribosomal protein-Mdm2-p53 pathway. Oncogene *29*, 4253-4260.

Delaney, J.R., Murakami, C.J., Olsen, B., Kennedy, B.K., and Kaeberlein, M. (2011). Quantitative evidence for early life fitness defects from 32 longevity-associated alleles in yeast. Cell Cycle *10*, 156-165.

Derenzini, M., and Ploton, D. (1991). Interphase nucleolar organizer regions in cancer cells. Int Rev Exp Pathol *32*, 149-192.

Dokal, I. (2000). Dyskeratosis congenita in all its forms. Br J Haematol *110*, 768-779.

Dragon, F., Gallagher, J.E., Compagnone-Post, P.A., Mitchell, B.M., Porwancher, K.A., Wehner, K.A., Wormsley, S., Settlage, R.E., Shabanowitz, J., Osheim, Y.*, et al.* (2002). A large nucleolar U3 ribonucleoprotein required for 18S ribosomal RNA biogenesis. Nature *417*, 967-970.

Emre, N.C., Ingvarsdottir, K., Wyce, A., Wood, A., Krogan, N.J., Henry, K.W., Li, K., Marmorstein, R., Greenblatt, J.F., Shilatifard, A.*, et al.* (2005). Maintenance of low histone ubiquitiylation by Ubp10p correlates with telomere-proximal Sir2 association and gene silencing. Molecular Cell *17*, 585-594.

Endo, A., Kitamura, N., and Komada, M. (2009). Nucleophosmin/B23 regulates ubiquitin dynamics in nucleoli by recruiting deubiquitylating enzyme USP36. J Biol Chem *284*, 27918-27923.

Finley, D., Sadis, S., Monia, B.P., Boucher, P., Ecker, D.J., Crooke, S.T., and Chau, V. (1994). Inhibition of proteolysis and cell cycle progression in a multiubiquitination-deficient yeast mutant. Mol Cell Biol *14*, 5501-5509.

Gallagher, J.E., Dunbar, D.A., Granneman, S., Mitchell, B.M., Osheim, Y., Beyer, A.L., and Baserga, S.J. (2004). RNA polymerase I transcription and pre-rRNA processing are linked by specific SSU processome components. Genes Dev *18*, 2506-2517.

Gardner, R.G., Nelson, Z., and Gottschling, D.E. (2005a). Degradation-mediated protein quality control in the nucleus. Cell *120*, 803-815.

Gardner, R.G., Nelson, Z.W., and Gottschling, D.E. (2005b). Ubp10/Dot4p regulates the persistence of ubiquitinated histone H2B: distinct roles in telomeric silencing and general chromatin. Mol Cell Biol *25*, 6123-6139.

Grandi, P., Rybin, V., Bassler, J., Petfalski, E., Strauss, D., Marzioch, M., Schafer, T., Kuster, B., Tschochner, H., Tollervey, D.*, et al.* (2002). 90S pre-ribosomes include the 35S pre-rRNA, the U3 snoRNP, and 40S subunit processing factors but predominantly lack 60S synthesis factors. Mol Cell *10*, 105-115.

Graner, E., Tang, D., Rossi, S., Baron, A., Migita, T., Weinstein, L.J., Lechpammer, M., Huesken, D., Zimmermann, J., Signoretti, S.*, et al.* (2004). The isopeptidase USP2a regulates the stability of fatty acid synthase in prostate cancer. Cancer Cell *5*, 253-261.

Grisendi, S., Mecucci, C., Falini, B., and Pandolfi, P.P. (2006). Nucleophosmin and cancer. Nat Rev Cancer *6*, 493-505.

Guthrie, C., and Fink, G.R. (1991). Guide to yeast genetics and molecular biology. Methods Enzymol *194*, 1-863.

Guthrie, C., Nashimoto, H., and Nomura, M. (1969). Structure and function of E. coli ribosomes. 8. Cold-sensitive mutants defective in ribosome assembly. Proc Natl Acad Sci U S A *63*, 384-391.

Haase, S.B., and Reed, S.I. (2002). Improved flow cytometric analysis of the budding yeast cell cycle. Cell Cycle *1*, 132-136.

Henras, A.K., Soudet, J., Gerus, M., Lebaron, S., Caizergues-Ferrer, M., Mougin, A., and Henry, Y. (2008). The post-transcriptional steps of eukaryotic ribosome biogenesis. Cell Mol Life Sci *65*, 2334-2359.

Henry, K.W., Wyce, A., Lo, W.S., Duggan, L.J., Emre, N.C., Kao, C.F., Pillus, L., Shilatifard, A., Osley, M.A., and Berger, S.L. (2003). Transcriptional activation via sequential histone H2B ubiquitylation and deubiquitylation, mediated by SAGA-associated Ubp8. Genes Dev *17*, 2648-2663.

James, P., Halladay, J., and Craig, E.A. (1996). Genomic libraries and a host strain designed for highly efficient two-hybrid selection in yeast. Genetics *144*, 1425-1436.

Kahana, A., and Gottschling, D.E. (1999). DOT4 links silencing and cell growth in Saccharomyces cerevisiae. Mol Cell Biol *19*, 6608-6620.

Kao, C.F., Hillyer, C., Tsukuda, T., Henry, K., Berger, S., and Osley, M.A. (2004). Rad6 plays a role in transcriptional activation through ubiquitylation of histone H2B. Genes Dev *18*, 184-195.

Keller, A., Nesvizhskii, A.I., Kolker, E., and Aebersold, R. (2002). Empirical statistical model to estimate the accuracy of peptide identifications made by MS/MS and database search. Anal Chem *74*, 5383-5392.

Korgaonkar, C., Hagen, J., Tompkins, V., Frazier, A.A., Allamargot, C., Quelle, F.W., and Quelle, D.E. (2005). Nucleophosmin (B23) targets ARF to nucleoli and inhibits its function. Mol Cell Biol *25*, 1258-1271.

Kouranti, I., McLean, J.R., Feoktistova, A., Liang, P., Johnson, A.E., Roberts-Galbraith, R.H., and Gould, K.L. (2010). A global census of fission yeast deubiquitinating enzyme localization and interaction networks reveals distinct compartmentalization profiles and overlapping functions in endocytosis and polarity. PLoS Biol *8*.

Krogan, N.J., Cagney, G., Yu, H., Zhong, G., Guo, X., Ignatchenko, A., Li, J., Pu, S., Datta, N., Tikuisis, A.P.*, et al.* (2006). Global landscape of protein complexes in the yeast Saccharomyces cerevisiae. Nature *440*, 637-643.

Krogan, N.J., Lam, M.H., Fillingham, J., Keogh, M.C., Gebbia, M., Li, J., Datta, N., Cagney, G., Buratowski, S., Emili, A.*, et al.* (2004a). Proteasome involvement in the repair of DNA double-strand breaks. Mol Cell *16*, 1027-1034.

Krogan, N.J., Peng, W.T., Cagney, G., Robinson, M.D., Haw, R., Zhong, G., Guo, X., Zhang, X., Canadien, V., Richards, D.P.*, et al.* (2004b). High-definition macromolecular composition of yeast RNA-processing complexes. Mol Cell *13*, 225-239.

Kuhn, C.D., Geiger, S.R., Baumli, S., Gartmann, M., Gerber, J., Jennebach, S., Mielke, T., Tschochner, H., Beckmann, R., and Cramer, P. (2007). Functional architecture of RNA polymerase I. Cell *131*, 1260-1272.

Kvint, K., Uhler, J.P., Taschner, M.J., Sigurdsson, S., Erdjument-Bromage, H., Tempst, P., and Svejstrup, J.Q. (2008). Reversal of RNA polymerase II ubiquitylation by the ubiquitin protease Ubp3. Mol Cell *30*, 498-506.

Lane, B.G., Ofengand, J., and Gray, M.W. (1995). Pseudouridine and O2'-methylated nucleosides. Significance of their selective occurrence in rRNA domains that function in ribosome-catalyzed synthesis of the peptide bonds in proteins. Biochimie *77*, 7-15.

Li, J., Olson, L.M., Zhang, Z., Li, L., Bidder, M., Nguyen, L., Pfeifer, J., and Rader, J.S. (2008). Differential display identifies overexpression of the USP36 gene, encoding a deubiquitinating enzyme, in ovarian cancer. Int J Med Sci *5*, 133-142.

Li, L., and Ye, K. (2006). Crystal structure of an H/ACA box ribonucleoprotein particle. Nature *443*, 302-307.

Liang, B., Zhou, J., Kahen, E., Terns, R.M., Terns, M.P., and Li, H. (2009). Structure of a functional ribonucleoprotein pseudouridine synthase bound to a substrate RNA. Nat Struct Mol Biol *16*, 740-746.

Licklider, L.J., Thoreen, C.C., Peng, J., and Gygi, S.P. (2002). Automation of nanoscale microcapillary liquid chromatography-tandem mass spectrometry with a vented column. Anal Chem *74*, 3076-3083.

Lim, Y.H., Charette, J.M., and Baserga, S.J. (2011). Assembling a protein-protein interaction map of the SSU processome from existing datasets. PLoS One *6*, e17701.

Lindstrom, M.S., and Zhang, Y. (2008). Ribosomal protein S9 is a novel B23/NPM-binding protein required for normal cell proliferation. J Biol Chem *283*, 15568-15576.

Marfany, G., and Denuc, A. (2008). To ubiquitinate or to deubiquitinate: it all depends on the partners. Biochem Soc Trans *36*, 833-838.

Meier, U.T. (2005). The many facets of H/ACA ribonucleoproteins. Chromosoma *114*, 1-14.

Memet, S., Gouy, M., Marck, C., Sentenac, A., and Buhler, J.M. (1988). RPA190, the gene coding for the largest subunit of yeast RNA polymerase A. J Biol Chem *263*, 2830-2839.

Mereau, A., Fournier, R., Gregoire, A., Mougin, A., Fabrizio, P., Luhrmann, R., and Branlant, C. (1997). An in vivo and in vitro structure-function analysis of the Saccharomyces cerevisiae U3A snoRNP: protein-RNA contacts and base-pair interaction with the pre-ribosomal RNA. J Mol Biol *273*, 552-571.

Montanaro, L., Trere, D., and Derenzini, M. (2008). Nucleolus, ribosomes, and cancer. Am J Pathol *173*, 301-310.

Ng, H.H., Ciccone, D.N., Morshead, K.B., Oettinger, M.A., and Struhl, K. (2003). Lysine-79 of histone H3 is hypomethylated at silenced loci in yeast and mammalian cells: a potential mechanism for position-effect variegation. Proc Natl Acad Sci U S A *100*, 1820-1825.

Ng, H.H., Feng, Q., Wang, H., Erdjument-Bromage, H., Tempst, P., Zhang, Y., and Struhl, K. (2002a). Lysine methylation within the globular domain of histone H3 by Dot1 is important for telomeric silencing and Sir protein association. Genes Dev *16*, 1518-1527.

Ng, H.H., Xu, R.M., Zhang, Y., and Struhl, K. (2002b). Ubiquitination of histone H2B by Rad6 is required for efficient Dot1-mediated methylation of histone H3 lysine 79. J Biol Chem *277*, 34655-34657.

Noma, K., and Grewal, S.I. (2002). Histone H3 lysine 4 methylation is mediated by Set1 and promotes maintenance of active chromatin states in fission yeast. Proc Natl Acad Sci U S A *99 Suppl 4*, 16438-16445.

Orlandi, I., Bettiga, M., Alberghina, L., and Vai, M. (2004). Transcriptional profiling of ubp10 null mutant reveals altered subtelomeric gene expression and insurgence of oxidative stress response. J Biol Chem *279*, 6414-6425.

Palladino, F., Laroche, T., Gilson, E., Axelrod, A., Pillus, L., and Gasser, S.M. (1993). SIR3 and SIR4 proteins are required for the positioning and integrity of yeast telomeres. Cell *75*, 543-555.

Paulson, H.L., Das, S.S., Crino, P.B., Perez, M.K., Patel, S.C., Gotsdiner, D., Fischbeck, K.H., and Pittman, R.N. (1997). Machado-Joseph disease gene product is a cytoplasmic protein widely expressed in brain. Ann Neurol *41*, 453-462.

Pestov, D.G., Lapik, Y.R., and Lau, L.F. (2008). Assays for ribosomal RNA processing and ribosome assembly. Curr Protoc Cell Biol *Chapter 22*, Unit 22 11.

Pestov, D.G., Strezoska, Z., and Lau, L.F. (2001). Evidence of p53-dependent cross-talk between ribosome biogenesis and the cell cycle: effects of nucleolar protein Bop1 on G(1)/S transition. Mol Cell Biol *21*, 4246-4255.

Philippi, A., Steinbauer, R., Reiter, A., Fath, S., Leger-Silvestre, I., Milkereit, P., Griesenbeck, J., and Tschochner, H. (2010). TOR-dependent reduction in the expression level of Rrn3p lowers the activity of the yeast RNA Pol I machinery, but does not account for the strong inhibition of rRNA production. Nucleic Acids Res *38*, 5315-5326.

Phipps, K.R., Charette, J.M., and Baserga, S.J. (2011). The SSU Processome in Ribosome Biogenesis - Progress and Prospects. WIREs RNA *2*, 1-21.

Rashid, R., Liang, B., Baker, D.L., Youssef, O.A., He, Y., Phipps, K., Terns, R.M., Terns, M.P., and Li, H. (2006). Crystal structure of a Cbf5-Nop10-Gar1 complex and implications in RNA-guided pseudouridylation and dyskeratosis congenita. Mol Cell *21*, 249-260.

Rauch, A., Bellew, M., Eng, J., Fitzgibbon, M., Holzman, T., Hussey, P., Igra, M., Maclean, B., Lin, C.W., Detter, A.*, et al.* (2006). Computational Proteomics Analysis System (CPAS): an extensible, open-source analytic system for evaluating and publishing proteomic data and high throughput biological experiments. J Proteome Res *5*, 112-121.

Raue, H.A., Klootwijk, J., and Musters, W. (1988). Evolutionary conservation of structure and function of high molecular weight ribosomal RNA. Prog Biophys Mol Biol *51*, 77-129.

Reichow, S.L., Hamma, T., Ferre-D'Amare, A.R., and Varani, G. (2007). The structure and function of small nucleolar ribonucleoproteins. Nucleic Acids Res *35*, 1452-1464.

Reyes-Turcu, F.E., Ventii, K.H., and Wilkinson, K.D. (2009). Regulation and cellular roles of ubiquitin-specific deubiquitinating enzymes. Annu Rev Biochem *78*, 363-397.

Robinson, M.D., Grigull, J., Mohammad, N., and Hughes, T.R. (2002). FunSpec: a web-based cluster interpreter for yeast. BMC Bioinformatics *3*, 35.

Robzyk, K., Recht, J., and Osley, M.A. (2000). Rad6-dependent ubiquitination of histone H2B in yeast. Science *287*, 501-504.

Rosenbaum, J.C., Fredrickson, E.K., Oeser, M.L., Garrett-Engele, C.M., Locke, M.N., Richardson, L.A., Nelson, Z.W., Hetrick, E.D., Milac, T.I., Gottschling, D.E., *et al.* (2011). Disorder targets misorder in nuclear quality control degradation: a disordered ubiquitin ligase directly recognizes its misfolded substrates. Mol Cell *41*, 93-106.

Ruggero, D., Grisendi, S., Piazza, F., Rego, E., Mari, F., Rao, P.H., Cordon-Cardo, C., and Pandolfi, P.P. (2003). Dyskeratosis congenita and cancer in mice deficient in ribosomal RNA modification. Science *299*, 259-262.

Russell, J., and Zomerdijk, J.C. (2005). RNA-polymerase-I-directed rDNA transcription, life and works. Trends Biochem Sci *30*, 87-96.

Russell, J., and Zomerdijk, J.C. (2006). The RNA polymerase I transcription machinery. Biochem Soc Symp, 203-216.

Savkur, R.S., and Olson, M.O. (1998). Preferential cleavage in pre-ribosomal RNA byprotein B23 endoribonuclease. Nucleic Acids Res *26*, 4508-4515.

Schaefer, J.B., and Morgan, D.O. (2011). Protein-linked ubiquitin chain structure restricts activity of deubiquitinating enzymes. J Biol Chem *286*, 45186-45196.

Singer, M.S., Kahana, A., Wolf, A.J., Meisinger, L.L., Peterson, S.E., Goggin, C., Mahowald, M., and Gottschling, D.E. (1998). Identification of high-copy disruptors of telomeric silencing in Saccharomyces cerevisiae. Genetics *150*, 613-632.

Smoot, M.E., Ono, K., Ruscheinski, J., Wang, P.L., and Ideker, T. (2011). Cytoscape 2.8: new features for data integration and network visualization. Bioinformatics *27*, 431-432.

Sowa, M.E., Bennett, E.J., Gygi, S.P., and Harper, J.W. (2009). Defining the human deubiquitinating enzyme interaction landscape. Cell *138*, 389-403.

Spence, J., Sadis, S., Haas, A.L., and Finley, D. (1995). A ubiquitin mutant with specific defects in DNA repair and multiubiquitination. Mol Cell Biol *15*, 1265-1273.

Steffen, K.K., MacKay, V.L., Kerr, E.O., Tsuchiya, M., Hu, D., Fox, L.A., Dang, N., Johnston, E.D., Oakes, J.A., Tchao, B.N.*, et al.* (2008). Yeast life span extension by depletion of 60s ribosomal subunits is mediated by Gcn4. Cell *133*, 292-302.

Sun, X.X., Dai, M.S., and Lu, H. (2007). 5-fluorouracil activation of p53 involves an MDM2-ribosomal protein interaction. J Biol Chem *282*, 8052-8059.

Sun, Z.W., and Allis, C.D. (2002). Ubiquitination of histone H2B regulates H3 methylation and gene silencing in yeast. Nature *418*, 104-108.

Sutherland, B.W., Toews, J., and Kast, J. (2008). Utility of formaldehyde cross-linking and mass spectrometry in the study of protein-protein interactions. J Mass

Spectrom *43*, 699-715.

Tarassov, K., Messier, V., Landry, C.R., Radinovic, S., Serna Molina, M.M., Shames, I., Malitskaya, Y., Vogel, J., Bussey, H., and Michnick, S.W. (2008). An in vivo map of the yeast protein interactome. Science *320*, 1465-1470.

Treiber, D.K., and Williamson, J.R. (2001). Beyond kinetic traps in RNA folding. Curr Opin Struct Biol *11*, 309-314.

Tsang, C.K., Bertram, P.G., Ai, W., Drenan, R., and Zheng, X.F. (2003). Chromatin-mediated regulation of nucleolar structure and RNA Pol I localization by TOR. Embo J *22*, 6045-6056.

van Leeuwen, F., Gafken, P.R., and Gottschling, D.E. (2002). Dot1p modulates silencing in yeast by methylation of the nucleosome core. Cell *109*, 745-756.

Vanrobays, E., Gleizes, P.E., Bousquet-Antonelli, C., Noaillac-Depeyre, J., Caizergues-Ferrer, M., and Gelugne, J.P. (2001). Processing of 20S pre-rRNA to 18S ribosomal RNA in yeast requires Rrp10p, an essential non-ribosomal cytoplasmic protein. Embo J *20*, 4204-4213.

Venema, J., and Tollervey, D. (1999). Ribosome synthesis in Saccharomyces cerevisiae. Annu Rev Genet *33*, 261-311.

Wang, C., Query, C.C., and Meier, U.T. (2002). Immunopurified small nucleolar ribonucleoprotein particles pseudouridylate rRNA independently of their association with phosphorylated Nopp140. Mol Cell Biol *22*, 8457-8466.

Warner, J.R. (1999). The economics of ribosome biosynthesis in yeast. Trends Biochem Sci *24*, 437-440.

Watkins, N.J., Segault, V., Charpentier, B., Nottrott, S., Fabrizio, P., Bachi, A., Wilm, M., Rosbash, M., Branlant, C., and Luhrmann, R. (2000). A common core RNP structure shared between the small nucleoar box C/D RNPs and the spliceosomal U4 snRNP. Cell *103*, 457-466.

Wilkinson, K.D. (1997). Regulation of ubiquitin-dependent processes by deubiquitinating enzymes. FASEB J *11*, 1245-1256.

Wittmeyer, J., Joss, L., and Formosa, T. (1999). Spt16 and Pob3 of Saccharomyces cerevisiae form an essential, abundant heterodimer that is nuclear, chromatin-associated, and copurifies with DNA polymerase alpha. Biochemistry *38*, 8961-8971.

Wright, D.E., Wang, C.Y., and Kao, C.F. (2012). Histone ubiquitylation and chromatin dynamics. Front Biosci *17*, 1051-1078.

Xu, P., Duong, D.M., Seyfried, N.T., Cheng, D., Xie, Y., Robert, J., Rush, J., Hochstrasser, M., Finley, D., and Peng, J. (2009). Quantitative proteomics reveals the function of unconventional ubiquitin chains in proteasomal degradation. Cell *137*, 133-145.

Yamamoto, R.T., Nogi, Y., Dodd, J.A., and Nomura, M. (1996). RRN3 gene of Saccharomyces cerevisiae encodes an essential RNA polymerase I transcription factor which interacts with the polymerase independently of DNA template. Embo J *15*, 3964-3973.

Yoon, A., Peng, G., Brandenburger, Y., Zollo, O., Xu, W., Rego, E., and Ruggero, D. (2006). Impaired control of IRES-mediated translation in X-linked dyskeratosis congenita. Science *312*, 902-906.

APPENDIX I:
YEAST STRAINS AND PLASMIDS

Yeast strains

Strain Name	Alias	*Genotype*	Reference
BY4741		*met15Δ0, his3Δ1, ura3Δ0, leu2Δ2*	(Brachmann et al., 1998)
PJ-4a		*MAT **a**, trp1-Δ1, leu2-3,112, ura3-52, his3-200, gal4Δ, gal80Δ, GAL2-ADE2, LYS2::GAL1-HIS3, met2::GAL7-lacZ*	(James et al., 1996)
RGY311	UCC6184	RGY379 *ubp10Δ::KanMX::ubp10(C371S)-MT6::URA3*	(Gardner et al., 2005b)
RGY312	UCC6185	RGY379 *ubp10Δ::KanMX::ubp10Δ(94-250)-MT6::URA3*	(Gardner et al., 2005b)
RGY313	UCC6186	RGY379 *ubp10Δ::KanMX::UBP10-MT6::URA3*	(Gardner et al., 2005b)
RGY375	UCC6195	*HMLa, Mata, HMRa, cdc7-1, bar1, trp1-289, ura3-52, leu2-3,112, his6 HTAI-FLAG-HTB1*	(Gardner et al., 2005b)
RGY376	UCC6196	RGY375 *sir2Δ::LEU2*	(Gardner et al., 2005b)
RGY377	UCC6197	RGY375 *sir3Δ::LEU2*	(Gardner et al., 2005b)
RGY378	UCC6198	RGY375 *sir4Δ::LEU2*	(Gardner et al., 2005b)
RGY379	UCC6199	RGY375 *ubp10Δ::KanMX*	(Gardner et al., 2005b)
RGY1221		BY4741 *trp1Δ::LEU2*	

RGY1593		*MAT a /α ura3-52/ura3-52 lys2-801amber/+ ade2-101ochre/+ trp1-Δ63/+ his3-Δ200/+ leu2-Δ1/+ DOT4-GFP-KanMX/+ Nop58-dsRED/+*	(Kahana and Gottschling, 1999)
RGY4595		RGY1221 *ubp10Δ::NatMX*	
RGY4625		RGY1221 *NOP56-3HA::KanMX*	
RGY4626		RGY1221 *NOP58-3HA::KanMX*	
RGY4627		RGY1221 *PWP2-3HA::KanMX*	
RGY4653		*RPA190-3HA::KanMX, all ubiquitin genes 8XHistidine tagged*	
RGY4668		RGY4595 *ubp10Δ::NatMX, UBP10-3HSV::TRP1*	
RGY4671		RGY1221 *CBF5-3HA::KanMX*	
RGY4696		RGY4625 *NOP56-3HA::KanMX, ubp10Δ::NatMX*	
RGY4697		RGY4626 *NOP58-3HA::KanMX, ubp10Δ::NatMX*	
RGY4698		RGY4627 *PWP2-3HA::KanMX, ubp10Δ::NatMX*	
RGY4709		RGY4671 *CBF5-3HA::KanMX, ubp10Δ::NatMX*	
RGY4728		RGY4653 *ubp10Δ::NatMX*	
RGY4742		RGY1221 *RPA190-3HA::KanMX*	

RGY4750		RGY4742 *ubp10Δ::NatMX*	
RGY4803		RGY4750 *UBP10-3HSV::TRP1*	
RGY5045		RGY4750 *P^{UBP10}-USP36::URA3 (2μ plasmid)*	
RGY5101		BY4741 *SIR4-GFP::URA3 NOP58-dsRED::NatMX*	
RGY5114		PJ-4a *GAD::LEU2 (2μ plasmid) GBD-$UBP10^{C371S}$::TRP1 (YEp)*	
RGY5115		PJ-4a *GAD-DHR2::LEU2 (2μ plasmid) GBD-$UBP10^{C371S}$::TRP1 (YEp)*	
RGY5116		PJ-4a *GAD-UTP22::LEU2 (2μ plasmid) GBD-$UBP10^{C371S}$::TRP1 (YEp)*	
RGY5117		PJ-4a *GAD-SIR4(612-1358)::LEU2 (2μ plasmid) GBD-$UBP10^{C371S}$::TRP1 (YEp)*	
RGY5118		RGY4742 *RPA190-3HA::TRP1 (2μ plasmid)*	
RGY5119		RGY4750 *RPA190-3HA::TRP1 (2μ plasmid)*	
RGY5285		*RPA190-3HA::KanMX, all ubiquitin genes 8 X Histidine tagged, ubp10Δ, P^{UBP10}-USP36::URA3 (2μ plasmid)*	

Plasmids

Plasmid		Relevent genes	Reference
pRG67		*trp1Δ::LEU2*	
pRG116		*LEU2 2μ pACT-GW-attR*	
pRG616	pRS306-str4-1-MT6	*URA3 INT ubp10^{C371S}-MT6*	(Gardner et al., 2005b)
pRG617	pRS306-str4-5-MT6	*URA3 INT ubp10$^{\Delta 94-250}$-MT6*	(Gardner et al., 2005b)
pRG637		*URA3 INT STR4/DOT4-6Myc*	(Gardner et al., 2005b)
pRG898		*TRP1 YEp Gal4BD-UBP10^{C371S}*	
pRG1332		*LEU2 2μ Gal4AD-Sir4$^{(612-1358)}$*	
pRG1337		*NatMX INT NOP58-dsRed*	
pRG1738		*TRP1 INT UBP10-3HSV*	
pRG2490		*LEU2 2μ pACT-GW-t-DHR2*	
pRG3410		*URA3 INT SIR4-GFP*	
pRG3232		*TRP1 2μ RPA190-3HA*	
pRG3351		*LEU2 2μ pACT-GW-t-UTP10*	
pRG3352		*LEU2 2μ pACT-GW-t-UTP22*	
pRG3421		*URA3 2μ P^{UBP10}-USP36*	

APPENDIX II:
PROTIENS THAT IMMUNOPRECIPITATE WITH UBP10 AFTER FORMALDHYDE CROSSLINKING

Peptide prophet filter= 0.35
c = cytoplasm, er = endoplasmic reticulum, m = mitochondria, n = nucleus, nu = nucleolus, s = secretory pathway, v = vacuole

	no tag 1	no tag 2	no tag 3	tag1	tag 2	tag 3	no tag	tag	tag/no tag	T test	
Protein	Total	Total	Total	Total	Total	Total	Sum	Sum	Ratio	p value	
ACS2	0	2	2	5	6	6	4	17	4.25	0.0107	n
ADE3	0	0	1	1	4	4	1	9	9.00	0.1047	n, c
ASN2	1	0	0	1	3	3	1	7	7.00	0.0765	c
BFR2	0	0	0	0	2	2	0	4	8.16	0.1835	nu
BMH2	1	1	0	2	2	5	2	9	4.50	0.1341	n, c
CAM1	1	0	0	2	2	2	0	6	12.24	0.0377	c
CBF5	0	0	0	2	3	2	0	7	14.29	0.0198	nu
CDC48	1	0	0	0	3	2	1	5	5.00	0.2667	n, c
DBP2	1	0	0	5	13	3	1	21	21.00	0.1593	nu
DBP4	0	0	0	1	2	1	0	4	8.16	0.0572	nu
DBP9	0	0	0	0	3	1	0	4	8.16	0.2697	n/a
DHR2	0	0	0	9	15	11	0	35	71.43	0.0221	nu
DPH5	0	0	1	1	1	2	1	4	4.00	0.1012	c
DRS1	0	0	0	2	5	3	0	10	20.41	0.0634	nu
FPR3	0	0	0	2	3	4	0	9	18.37	0.0351	nu
FPR4	0	0	0	0	3	2	0	5	10.20	0.1994	nu
GCD11	0	0	1	3	3	4	1	10	10.00	0.0031	c
GCN1	0	0	0	1	2	1	0	4	8.16	0.0572	c
GLY1	0	0	2	2	2	2	2	6	3.00	0.1835	n, c
GND1	0	0	0	4	5	4	0	13	26.53	0.0059	c
HAS1	0	0	0	5	6	6	0	17	34.69	0.0034	nu
HRP1	0	0	0	1	1	2	0	4	8.16	0.0572	n
HTB2	0	1	0	1	2	2	1	5	5.00	0.0474	n
IMD4	0	0	0	4	0	4	0	8	16.33	0.1835	c
KRE33	0	0	0	2	5	2	0	9	18.37	0.0955	nu
LYS20/21	1	0	0	4	8	2	0	14	28.57	0.1288	n
MAK11	0	0	0	2	4	2	0	8	16.33	0.0572	nu
MAK21	0	0	0	1	4	1	0	6	12.24	0.1835	nu
MDN1	0	0	0	1	4	0	0	5	10.20	0.2999	n
MIR1	0	1	1	0	2	4	2	6	3.00	0.3685	m
MRD1	0	0	0	1	7	2	0	10	20.41	0.2143	nu
NCL1	0	0	0	1	2	1	0	4	8.16	0.0572	n
NOC2	0	0	0	1	3	3	0	7	14.29	0.0728	nu
NOG1	0	0	0	1	3	1	0	5	10.20	0.1296	n
NOP1	1	1	1	1	5	3	3	9	3.00	0.2254	nu
NOP12	0	0	0	2	2	1	0	5	10.20	0.0377	nu
NOP4	0	0	0	1	3	1	0	5	10.20	0.1296	nu
NOP56	1	1	0	4	6	3	2	13	6.50	0.0399	nu
NOP58	1	0	2	5	8	10	3	23	7.67	0.0310	nu

NOP7	0	0	0	0	2	2	0	4	8.16	0.1835	nu
NPL3	2	1	0	3	3	3	3	9	3.00	0.0742	n
NSR1	1	0	0	4	5	5	1	14	14.00	0.0008	nu
NUG1	0	0	0	0	3	1	0	4	8.16	0.2697	n, nu
POL5	0	0	0	0	1	3	0	4	8.16	0.2697	n, nu
PRP43	0	0	0	3	9	4	0	16	32.65	0.1028	nu
PWP1	0	0	0	1	2	1	0	4	8.16	0.0572	nu
PWP2	0	0	0	4	4	6	0	14	28.57	0.0198	nu
PYC2	0	0	0	1	1	2	0	4	8.16	0.0572	c
RNR2	0	1	0	1	2	3	1	6	6.00	0.0824	c
RNR4	0	0	0	1	1	2	0	4	8.16	0.0572	n
RPA190	0	0	2	4	9	3	2	16	8.00	0.1158	nu
RPL13B	0	0	0	0	0	8	0	8	16.33	0.4226	c
RPL18A	0	0	0	1	2	5	0	8	16.33	0.1567	c
RPL31A	1	1	1	2	3	4	3	9	3.00	0.0742	c
RPL6A	1	1	1	1	1	7	3	9	3.00	0.4226	c
RPL7A	0	1	0	13	1	0	1	14	14.00	0.4085	c
RPS1A	2	1	1	8	4	5	4	17	4.25	0.0600	c
RRP5	0	0	0	8	19	13	0	40	81.63	0.0524	nu
SEC13	0	0	0	1	2	1	0	4	8.16	0.0572	s
SEC4	0	0	0	1	2	3	0	6	12.24	0.0742	s
SEC53	1	0	0	0	3	5	1	8	8.00	0.2463	er
SIS1	0	0	0	1	0	3	0	4	8.16	0.2697	n, c
SPT16	0	0	0	0	6	0	0	6	12.24	0.4226	n
SUB2	0	0	0	2	4	3	0	9	18.37	0.0351	n
SUP45	1	0	0	1	2	1	1	4	4.00	0.1012	c
SWP82	0	1	0	2	0	3	1	5	5.00	0.2667	n
TKL1	3	3	3	7	10	11	9	28	3.11	0.0342	n
TY1B-BL	0	0	0	0	4	0	0	4	8.16	0.4226	n
UBP10	0	0	0	38	42	40	0	120	244.90	0.0008	nu, n, c
URA2	2	2	0	2	8	4	4	14	3.50	0.1908	c
URA5	0	0	0	0	2	2	0	4	8.16	0.1835	c
URA7	0	0	0	0	2	2	0	4	8.16	0.1835	c
UTP10	0	0	0	1	7	2	0	10	20.41	0.2143	nu
UTP13	0	0	0	2	2	4	0	8	16.33	0.0572	nu
UTP17	0	0	0	1	2	3	0	6	12.24	0.0742	nu
UTP22	0	0	0	5	8	7	0	20	40.82	0.0171	nu
UTP4	0	0	0	0	2	3	0	5	10.20	0.1994	nu
UTP7	0	0	0	1	1	2	0	4	8.16	0.0572	nu
VMA13	0	1	0	1	2	1	1	4	4.00	0.1012	v
YMR099C	0	0	0	1	1	3	0	5	10.20	0.1296	n
YOL077C	0	0	0	2	1	1	0	4	8.16	0.0572	nu, n
YOR051C	0	0	0	1	2	1	0	4	8.16	0.0572	n
YRA1	0	0	0	1	4	1	0	6	12.24	0.1835	n

APPENDIX III:

Proteins with increased abundance in the ubiquitin proteome from *ubp10*Δ cells

tech= technical replicate

Bold protein names denote nucleolar proteins

	***UBP10* biological 1**		***UBP10* biological 2**		***UBP10* biological 3**		***ubp10*Δ biological 1**		***ubp10*Δ biological 2**		***ubp10*Δ biological 3**		***UBP10***	***ubp10*Δ**	***ubp10*Δ /UBP10**	**Ttest**
	tech 1	**tech 2**	**tech 1**	**tech 2**	**tech 1**	**tech 2**	**tech 1**	**tech 2**	**tech 1**	**tech 2**	**tech 1**	**tech 2**				
Protein	**Total**	**Total**	**Total**	**Total**	**Total**	**Total**	**Total**	**Total**	**Total**	**Total**	**Total**	**Total**	**SUM**	**SUM**	**Ratio**	**p-value**
AIM2	0	0	0	1	0	0	2	1	0	1	0	1	1	5	5.00	0.094363368
ART5	7	6	7	9	6	7	10	3	14	13	11	13	42	64	1.52	0.077326088
AXL2	0	0	0	1	1	1	1	1	2	1	3	0	3	8	2.67	0.120886708
BAP3	0	0	0	0	0	1	1	0	7	1	1	4	1	14	14.00	0.10289472
BEM2	12	19	26	11	18	33	22	8	55	50	28	41	119	204	1.71	0.122188348
BUL1	2	4	4	5	3	1	7	2	10	6	2	6	19	33	1.74	0.137174715
CBF5	**0**	**0**	**0**	**0**	**0**	**0**	**2**	**0**	**0**	**0**	**1**	**1**	**0**	**4**	**400.00**	0.101939479
CHC1	4	8	7	3	6	16	10	1	32	18	13	28	44	102	2.32	0.1017513
CHS2	0	0	0	0	1	1	0	1	3	1	0	2	2	7	3.50	0.155001661
CIT2	1	0	3	2	1	7	3	0	9	10	4	10	14	36	2.57	0.105244083
COS1	0	0	0	0	0	0	0	0	5	3	0	3	0	11	1100.00	0.089589174
COS3	0	0	0	1	0	7	3	0	13	12	1	11	8	40	5.00	0.086933999
COS6	0	0	0	0	0	1	0	0	2	1	0	4	1	7	7.00	0.191975033
CRM1	1	1	1	1	1	2	2	1	6	3	1	2	7	15	2.14	0.143693046
DBP2	**0**	**0**	**0**	**0**	**1**	**0**	**1**	**0**	**1**	**1**	**1**	**2**	**1**	**6**	**6.00**	0.025041079
DSE1	0	1	1	0	1	1	0	0	3	3	2	3	4	11	2.75	0.114985844
ECM29	1	0	1	0	0	0	0	0	2	1	1	3	2	7	3.50	0.155001661
ECM8	0	1	0	0	0	0	2	0	2	0	0	1	1	5	5.00	0.170982498
ERG25	0	0	0	0	0	0	0	0	1	1	0	3	0	5	500.00	0.141234773
ERG27	0	0	0	0	0	0	0	0	2	1	0	2	0	5	500.00	0.092515006
ERG5	0	0	0	0	1	0	0	0	2	1	1	1	1	5	5.00	0.094363368
ERG6	0	0	0	1	1	3	1	1	3	2	1	2	5	10	2.00	0.186302689

	UBP10 **biological 1**		***UBP10*** **biological 2**		***UBP10*** **biological 3**		***ubp10*****Δ biological 1**		***ubp10*****Δ biological 2**		***ubp10*****Δ biological 3**		***UBP10***	***ubp10*****Δ**	***ubp10*****Δ*****/UBP10***	**Ttest**
	tech 1	**tech 2**	**tech 1**	**tech 2**	**tech 1**	**tech 2**	**tech 1**	**tech 2**	**tech 1**	**tech 2**	**tech 1**	**tech 2**				
Protein	**Total**	**Total**	**Total**	**Total**	**Total**	**Total**	**Total**	**Total**	**Total**	**Total**	**Total**	**Total**	**SUM**	**SUM**	**Ratio**	**p-value**
ETP1	0	0	0	1	0	1	1	0	1	2	1	4	2	9	4.50	0.097389175
FCY2	3	1	3	2	2	4	2	1	10	5	6	9	15	33	2.20	0.100419832
FPR3	**0**	**0**	**0**	**0**	**1**	**0**	**1**	**0**	**1**	**1**	**1**	**1**	**1**	**5**	**5.00**	0.017900123
FPR4	**0**	**0**	**0**	**0**	**0**	**0**	**2**	**1**	**0**	**1**	**0**	**1**	**0**	**5**	**500.00**	0.042193997
FPS1	0	0	0	0	0	0	1	0	2	2	0	0	0	5	500.00	0.092515006
FRE1	12	7	14	10	6	20	17	0	26	25	21	22	69	111	1.61	0.155823163
FTR1	1	0	1	1	0	0	1	0	2	1	3	2	3	9	3.00	0.07434228
GCN1	5	8	4	3	3	9	3	0	22	25	10	24	32	84	2.63	0.116303403
GLT1	0	0	1	0	1	3	3	0	7	1	4	4	5	19	3.80	0.075189718
GNP1	16	10	22	14	7	20	25	2	28	29	24	26	89	134	1.51	0.153768988
GTO3	0	0	0	0	0	0	0	0	1	2	1	1	0	5	500.00	0.042193997
HAS1	**0**	**0**	**0**	**0**	**0**	**0**	**1**	**0**	**1**	**2**	**0**	**0**	**0**	**4**	**400.00**	0.101939479
HHF1	0	0	0	0	0	0	0	0	1	1	0	3	0	5	500.00	0.141234773
HIP1	0	1	0	1	0	5	3	0	9	7	6	12	7	37	5.29	0.03470662
HNM1	0	0	0	0	0	0	0	0	2	1	1	1	0	5	500.00	0.042193997
HTB1/HTB2	**19**	**9**	**12**	**13**	**2**	**10**	**26**	**6**	**11**	**27**	**16**	**19**	**65**	**105**	**1.62**	0.136554389
HXT2	4	9	5	5	0	2	6	2	9	11	8	6	25	42	1.68	0.142115817
IKI3	0	0	0	0	0	2	0	0	2	2	1	2	2	7	3.50	0.142335055
KAP95	0	0	1	0	0	0	0	0	1	2	0	2	1	5	5.00	0.170982498
LSB5	0	0	0	0	0	0	0	0	1	1	0	2	0	4	400.00	0.101939479
LYP1	0	1	0	1	0	4	0	0	7	2	5	4	6	18	3.00	0.168411632
MAK21	**0**	**1**	**0**	**0**	**0**	**0**	**0**	**3**	**2**	**1**	**0**	**0**	**1**	**6**	**6.00**	0.175261118
MDN1	**1**	**0**	**0**	**0**	**0**	**0**	**0**	**0**	**3**	**1**	**1**	**1**	**1**	**6**	**6.00**	0.128576898
MMT2	3	0	1	1	0	7	5	2	13	9	12	11	12	52	4.33	0.011716235
MOT3	3	3	2	4	2	4	4	2	9	7	3	6	18	31	1.72	0.104471677
MSC2	1	1	5	5	2	6	7	1	13	9	7	11	20	48	2.40	0.042795686
MUP1	4	1	5	2	0	4	6	0	5	7	4	5	16	27	1.69	0.182560485
MYO2	0	0	0	1	1	2	0	1	3	2	3	1	4	10	2.50	0.128742648

	UBP10 **biological 1**		***UBP10*** **biological 2**		***UBP10*** **biological 3**		***ubp10*Δ biological 1**		***ubp10*Δ biological 2**		***ubp10*Δ biological 3**		***UBP10***	***ubp10*Δ**	***ubp10*Δ/*UBP10***	**Ttest**
	tech 1	**tech 2**	**tech 1**	**tech 2**	**tech 1**	**tech 2**	**tech 1**	**tech 2**	**tech 1**	**tech 2**	**tech 1**	**tech 2**				
Protein	**Total**	**Total**	**Total**	**Total**	**Total**	**Total**	**Total**	**Total**	**Total**	**Total**	**Total**	**Total**	**SUM**	**SUM**	**Ratio**	**p-value**
NBA1	0	1	0	0	0	1	1	1	1	2	1	0	2	6	3.00	0.074526623
NEW1	1	3	3	6	4	5	4	2	10	9	3	10	22	38	1.73	0.1558034
NIP1	1	1	2	1	0	3	2	0	7	3	2	9	8	23	2.88	0.139078609
NUG1	0	0	0	1	0	1	1	1	2	2	0	0	2	6	3.00	0.152502285
NUP170	0	0	0	0	1	0	0	1	5	3	0	1	1	10	10.00	0.122211053
OPT1	3	0	4	3	0	4	3	0	7	6	6	6	14	28	2.00	0.112250194
PBP1	17	21	32	34	26	39	33	32	59	105	61	57	169	347	2.05	0.040121435
PRM5	0	2	0	2	2	2	2	2	2	2	2	2	8	12	1.50	0.174687814
PTH2	3	2	1	0	2	2	3	2	3	3	3	3	10	17	1.70	0.039133898
RAD6	0	0	0	0	0	0	1	0	0	0	2	1	0	4	400.00	0.101939479
RPA190	**17**	**25**	**24**	**22**	**27**	**22**	**71**	**39**	**73**	**74**	**40**	**60**	**137**	**357**	**2.61**	0.002268151
RPL11B	3	2	1	1	0	0	4	0	4	4	3	6	7	21	3.00	0.037074366
RPL13A/B	1	1	0	0	0	0	12	3	4	4	4	5	2	32	16.00	0.013755897
RPL14B	1	3	1	3	2	1	2	5	10	7	2	11	11	37	3.36	0.039861564
RPL15A	1	1	1	1	1	0	1	0	4	2	1	3	5	11	2.20	0.161940307
RPL16A/B	0	0	1	0	2	1	5	1	5	7	4	6	4	28	7.00	0.003689453
RPL17A/B	0	1	1	1	0	0	6	0	4	7	3	5	3	25	8.33	0.014319858
RPL20A	4	1	2	2	0	3	10	5	7	10	7	10	12	49	4.08	0.000266237
RPL21A/B	2	1	0	1	0	0	4	1	5	6	3	7	4	26	6.50	0.007126771
RPL25	0	1	0	2	0	0	2	1	2	2	2	1	3	10	3.33	0.018873496
RPL27B	0	0	0	0	0	1	2	0	5	8	3	6	1	24	24.00	0.022508097
RPL3	0	1	0	0	0	1	1	0	3	2	0	2	2	8	4.00	0.106627647
RPL30	0	0	0	0	0	0	2	1	3	4	2	5	0	17	1700.00	0.005266289
RPL33A/B	1	1	1	1	1	1	7	0	2	4	1	3	6	17	2.83	0.130342412

	UBP10 biological 1		*UBP10* biological 2		*UBP10* biological 3		*ubp10*Δ biological 1		*ubp10*Δ biological 2		*ubp10*Δ biological 3		*UBP10*	*ubp10*Δ	*ubp10*Δ */UBP10*	Ttest
	tech 1	tech 2	tech 1	tech 2	tech 1	tech 2	tech 1	tech 2	tech 1	tech 2	tech 1	tech 2				
Protein	**Total**	**Total**	**Total**	**Total**	**Total**	**Total**	**Total**	**Total**	**Total**	**Total**	**Total**	**Total**	**SUM**	**SUM**	**Ratio**	**p-value**
RPL5	0	0	0	0	0	3	1	0	2	5	1	2	3	11	3.67	0.156565946
RPL6A/B	1	0	1	2	0	2	1	0	10	9	5	7	6	32	5.33	0.049657986
RPL7A	0	0	0	0	0	0	8	0	7	11	2	7	0	35	3500.00	0.017090669
RPL9A	0	0	0	0	0	0	0	0	4	3	2	6	0	15	1500.00	0.047602768
RPP0	0	2	3	1	1	1	2	2	2	4	3	4	8	17	2.13	0.027621513
RPP2B	0	0	0	0	0	0	0	0	1	0	2	1	0	4	400.00	0.101939479
RPS13	1	0	1	2	0	0	4	2	4	4	2	9	4	25	6.25	0.018870621
RPS14A	3	2	1	0	0	1	3	0	2	2	3	3	7	13	1.86	0.169257206
RPS15	0	0	0	0	0	0	1	0	1	2	2	2	0	8	800.00	0.010323415
RPS16A	0	0	0	0	0	0	1	0	6	1	0	3	0	11	1100.00	0.110283235
RPS17B	1	1	0	0	0	0	2	0	2	1	0	2	2	7	3.50	0.105499815
RPS18B	0	0	0	0	0	0	1	0	5	4	2	6	0	18	1800.00	0.026692591
RPS19B	0	0	0	0	0	0	0	0	2	1	1	3	0	7	700.00	0.058329303
RPS2	0	0	2	0	0	0	3	0	4	1	2	2	2	12	6.00	0.036942038
RPS22A	0	0	0	0	0	0	0	0	2	1	2	2	0	7	700.00	0.033532398
RPS25A	0	0	0	0	0	0	1	0	0	1	2	0	0	4	400.00	0.101939479
RPS3	4	4	7	4	2	8	12	3	19	17	12	18	29	81	2.79	0.01432253
RPS4A	5	2	6	2	2	5	15	0	23	32	17	26	22	113	5.14	0.019709461
RPS6B	2	2	7	2	0	4	12	0	10	14	3	8	17	47	2.76	0.076786229
RPS8A	1	2	4	2	2	9	12	0	11	14	6	9	20	52	2.60	0.055565324
RPS9B	0	0	0	0	0	0	3	2	3	4	1	4	0	17	1700.00	0.001935836
RRP12	**0**	**0**	**0**	**0**	**0**	**0**	**0**	**1**	**1**	**2**	**1**	**0**	**0**	**5**	**500.00**	0.042193997
SAM3	0	1	3	0	0	2	6	0	4	6	2	5	6	23	3.83	0.035321263
SCP160	9	10	7	7	15	17	10	9	27	24	12	25	65	107	1.65	0.106531395
SDA1	0	0	0	0	0	0	0	0	2	0	0	2	0	4	400.00	0.174687814
SEC21	0	0	0	0	0	2	0	0	6	8	1	3	2	18	9.00	0.110269787
SIK1	0	0	0	0	0	0	0	0	1	0	2	4	0	7	700.00	0.13454092
SIT1	0	0	0	0	0	1	0	0	2	2	1	3	1	8	8.00	0.065827959
SLM1	0	0	0	1	0	1	0	0	1	2	1	3	2	7	3.50	0.155001661

	***UBP10* biological 1**		***UBP10* biological 2**		***UBP10* biological 3**		***ubp10*Δ biological 1**		***ubp10*Δ biological 2**		***ubp10*Δ biological 3**		***UBP10***	***ubp10*Δ**	***ubp10*Δ/*UBP10***	**Ttest**
	tech 1	**tech 2**	**tech 1**	**tech 2**	**tech 1**	**tech 2**	**tech 1**	**tech 2**	**tech 1**	**tech 2**	**tech 1**	**tech 2**				
Protein	**Total**	**Total**	**Total**	**Total**	**Total**	**Total**	**Total**	**Total**	**Total**	**Total**	**Total**	**Total**	**SUM**	**SUM**	**Ratio**	**p-value**
SMF1	0	0	0	1	0	3	1	0	3	6	4	5	4	19	4.75	0.0490909
SNF1	73	67	72	79	64	111	79	35	211	158	149	145	466	777	1.67	0.100083314
SRP40	0	0	1	1	1	3	2	0	3	5	2	5	6	17	2.83	0.079145634
STE4	1	0	0	0	0	1	0	0	1	2	2	2	2	7	3.50	0.105499815
STE6	4	5	4	3	2	7	4	1	14	13	5	15	25	52	2.08	0.130525748
SXM1	0	1	0	1	0	1	1	0	5	3	1	3	3	13	4.33	0.077899251
TAL1	1	0	0	0	0	1	0	0	1	2	2	3	2	8	4.00	0.106627647
TDP1	0	0	0	0	0	0	1	0	2	1	1	2	0	7	700.00	0.012676602
TEL1	0	0	0	0	0	2	0	1	3	1	4	3	2	12	6.00	0.049790066
TNA1	0	0	1	0	0	3	1	0	6	5	3	6	4	21	5.25	0.04508842
TPI1	0	0	0	0	0	1	0	0	2	0	1	3	1	6	6.00	0.175261118
TY1B-DR1	0	0	1	1	0	0	1	0	7	7	0	0	2	15	7.50	0.192241138
UBC1	5	5	4	5	0	5	8	1	10	7	11	12	24	49	2.04	0.053458388
UBC13	3	3	2	2	0	1	7	0	4	5	2	3	11	21	1.91	0.172515395
UBC8	2	2	2	0	0	1	1	0	3	3	5	3	7	15	2.14	0.144748684
URB1	0	0	0	0	0	0	0	0	2	1	0	1	0	4	400.00	0.101939479
UTP10	**0**	**1**	**0**	**0**	**0**	**0**	**0**	**0**	**3**	**0**	**1**	**2**	**1**	**6**	**6.00**	0.175261118
VAS1	0	3	4	9	6	20	7	3	24	22	17	19	42	92	2.19	0.094222069
VMA13	0	0	0	1	0	0	2	0	0	1	1	1	1	5	5.00	0.094363368
VTC4	5	1	5	2	2	9	9	0	22	14	15	12	24	72	3.00	0.043631905
WBP1	0	0	0	0	0	0	0	0	2	2	0	2	0	6	600.00	0.075586818
YAR009C	0	0	0	0	0	0	0	0	0	0	3	3	0	6	600.00	0.174687814
YBR238C	1	4	4	1	2	14	4	2	25	21	16	22	26	90	3.46	0.04629129
YDJ1	0	1	0	2	2	1	2	0	3	3	4	4	6	16	2.67	0.04754151
YDR222W	0	0	0	0	0	0	0	0	1	3	0	4	0	8	800.00	0.121188084
YEH1	0	0	0	0	1	1	0	0	3	2	0	2	2	7	3.50	0.198729458
YFR006W	2	1	0	1	1	3	1	2	3	3	5	4	8	18	2.25	0.0442042

	UBP10 **biological 1**		***UBP10*** **biological 2**		***UBP10*** **biological 3**		***ubp10*****Δ biological 1**		***ubp10*****Δ biological 2**		***ubp10*****Δ biological 3**		***UBP10***	***ubp10*****Δ**	***ubp10*****Δ*****/UBP10***	**Ttest**
	tech 1	**tech 2**	**tech 1**	**tech 2**	**tech 1**	**tech 2**	**tech 1**	**tech 2**	**tech 1**	**tech 2**	**tech 1**	**tech 2**				
Protein	**Total**	**Total**	**Total**	**Total**	**Total**	**Total**	**Total**	**Total**	**Total**	**Total**	**Total**	**Total**	**SUM**	**SUM**	**Ratio**	**p-value**
YGR130C	0	2	0	0	2	2	0	2	2	3	3	3	6	13	2.17	0.104911149
YHR131C	0	0	0	0	0	3	1	0	1	4	1	3	3	10	3.33	0.172900201
YIP5	0	0	0	0	0	0	0	0	1	2	1	0	0	4	400.00	0.101939479
YJR015W	0	0	0	0	0	0	0	0	2	1	1	1	0	5	500.00	0.042193997
YMR160W	3	9	5	4	5	11	10	2	16	13	10	16	37	67	1.81	0.078574904
YNR061C	0	0	1	0	0	0	1	0	1	1	0	1	1	4	4.00	0.094017029
YOL019W	1	2	3	2	3	1	3	6	3	3	2	3	12	20	1.67	0.077947151
YPT1	0	0	1	0	0	1	1	0	3	0	4	4	2	12	6.00	0.085320254
ZEO1	0	0	0	0	0	0	0	0	2	1	1	0	0	4	400.00	0.101939479
ZRC1	0	1	0	1	0	0	1	0	1	1	1	1	2	5	2.50	0.094017029
ZRT1	2	1	1	0	2	2	3	0	4	2	4	5	8	18	2.25	0.076539282

CURRICULUM VITAE

EDUCATION

Doctoral of Philosophy, Pharmacology, 2006 - 2012
Advanced to Candidacy, November 2008
University of Washington, Seattle, WA.

Bachelor of Science, Biochemistry and Molecular Biology, 2002 – 2006
University of California, Davis. Davis, CA.

HONORS/AWARDS

- Instituational Training Grant for Pharmacological Sciences, 2007 – 2010
- Best Poster Award in Biological and Medical Applications, Protein Degradation Pathways in Health and Disease Conference, January 2012

RESEARCH EXPERIENCE

Ph.D Candidate, Department of Pharmacology, University of Washington, Seattle, WA, September 2006 – March 2012

- Elucidating novel roles for the yeast deubiquitinase Ubp10. Using genetic, proteomic, biochemical and molecular biological techniques, I identified Ubp10 as a critical regulator of ribosome biogenesis through the deubiquitination of a novel substrate. The substrate, the large subunit of RNA Polymerase I, is rapidly degraded in the absence of Ubp10, leading to a decreased production of rRNA and ribosomes, which leads to slowed growth. I also discovered the human homolog of Ubp10, USP36, and found that it is able to functionally rescue the *ubp10*Δ phenotype.
- Advisor: Rich Gardner, Ph.D.

Undergraduate Researcher, Department of Anatomy, Physiology and Cell Biology, University of California, Davis, CA, November 2003 - June 2006

- Conducted research on the molecular mechanisms of airways remodeling in response to air pollutants from cigarette smoke. Specifically, I investigated if a lung-specific isoform of cytochrome P450 was inhibited by naphthalene.
- Advisor: Laura Van Winkle, Ph.D.

Research Intern: Physcial and Analytical Chemistry, Bend Research Inc., Bend, OR. Summers of 2003, 2004, and 2005.

- Bend Research Inc. is a privately held company that specializes in the research and development of novel pharmaceutical-delivery

technologies. During my three summers working there I used advanced technologies such as High Performance Liquid Chromatography, Scanning Electron Microscopy and Differential Scanning Calorimetry to assess the stability and purity of drugs to determine proper dosing formulations.
- Advisor: Rod Ray, Ph.D.

TEACHING

Teaching Assistant, Department of Pharmacology, Univeristy of Washington, Seattle, WA. Septemeber 2007 – March 2008
- Advised undergraduate General Pharmacology 401 and 402 students during office hours.
- Led weekly discussion sections for undergraduates.
- Graded exams and assignments.

PUBLICATIONS

Richardson LA, Reed BJ, Freed EM, Charette MJ, Locke MN, Milac TI, Baserga SJ, and Gardner RG. A conserved deubiquitinating enzyme controls cell growth by regulating RNA polymerase I stability. Manuscript submitted for review.

Rosenbaum JC, Fredrickson EK, Oeser ML, Garrett-Engele CM, Locke MN, **Richardson LA**, Nelson ZW, Hetrick ED, Milac TI, Gottschling DE, Gardner RG. (2011) Disorder targets misorder in nuclear quality control degradation: a disordered ubiquitin ligase directly recognizes its misfolded substrates. Mol Cell *41*:93–106.

ABSTRACTS/POSTERS PRESENTATIONS

Richardson LA, Gardner RG. Identifying novel roles for the yeast deubiquitinase Ubp10. Poster session presented at: 2009 CSHL Meeting on Yeast Cell Biology; 2009 Aug 11-15; Cold Spring Harbor, NY. USA.

Richardson LA, Gardner RG. Identifying novel roles for the yeast deubiquitinase Ubp10. Poster session presented at: Yeast Genetics 2010; 2010 July 27- Aug 1; Vancouver, BC. Canada.

Richardson LA, Gardner RG. A conserved deubiquitinating enzyme controls cell growth by regulating RNA polymerase I stability. Poster session presented at: PPDUP 2012; 2012 Jan 22- 25; San Diego, CA. USA.